MTech (Power Electronics and Systems)

Udeesha Gaur

2026

PERFORMANCE ANALYSIS AND MODELLING OF T-TYPE DUAL ACTIVE BRIDGE AND CUK-PFC CONVERTER USED IN EV CHARGING

A DISSERTION
SUBMITTED IN PARTIAL FULFILLMENT OF THE REQUIREMENTS
FOR THE AWARD OF THE DEGREE
OF

MASTER OF TECHNOLOGY
IN
POWER ELECTRONICS AND SYSTEMS

Submitted by:

UDEESHA GAUR

(24/PES/24)

Under the Supervision of:

PROF. ALKA SINGH

DR. ANKITA MATTA

DEPARTMENT OF ELECTRICAL ENGINEERING

DELHI TECHNOLOGICAL UNIVESITY

(Formerly Delhi College of Engineering)

Bawana Road, New Delhi, 110042

MAY, 2026

DELHI TECHNOLOGICAL UNIVERSITY

(Formerly Delhi College of Engineering)

Shahbad Daulatpur, Bawana Road, New Delhi-110042

CANDIDATE'S DECLARATION

I, Udeesha Gaur, Roll No. 2K24/PES/24, student of MTech (Power Electronics & Systems), hereby declare that the project Dissertation titled "Performance Analysis and Modelling of T-Type Dual Active Bridge and Cuk-PFC Converter Used in EV Charging" which is submitted by me to the Department of Electrical Engineering, Delhi Technological University, Delhi in partial fulfillment of the requirement for the award of the degree of Master of Technology, is original and not copied from any source without proper citation. This work has not previously formed the basis for the award of any Degree, Diploma Associateship, Fellowship or other similar title or recognition.

Place: Delhi

Date:

Udeesha Gaur

2K24/PES/24

DEPARTMENT OF ELECTRICAL ENGINEERING
DELHI TECHNOLOGICAL UNIVERSITY
(Formerly Delhi College of Engineering)
Shahbad Daulatpur, Bawana Road, New Delhi-110042

CERTIFICATE

I hereby certify that the Project Dissertation titled "Performance Analysis and Modelling of T-Type Dual Active Bridge and Cuk-PFC Converter Used in EV Charging" which is submitted by Udeesha Gaur, Roll No. 2K24/PES/24, Department of Electrical Engineering, Delhi Technological University, Delhi in partial fulfillment of the requirement for the award of the degree of Master of Technology, is a record of the project work carried out by the student under my supervision. To the best of my knowledge this work has not been submitted in part or full for any Degree or Diploma to this University or elsewhere.

Place: Delhi	**Prof. Alka Singh**	**Dr. Ankita Matta**
May 2026	Professor Department of Electrical Engineering (DTU, Delhi)	Assistant Professor Department of Electrical engineering (DTU, Delhi)

ACKNOWLEDGEMENT

I would like to take this opportunity to thank all those who helped in the successful completion of this thesis sincerely. First of all, I am thankful to my supervisors, Prof. Alka Singh & Mrs. Ankita Matta for their valuable guidance and constant support in this project. Their valuable suggestions and technical knowledge helped me to get through many difficulties in my research.

I would like to express my sincere thanks to the faculty members of the Department of Electrical Engineering, Delhi Technological University for their academic support and technical help, which was needed to complete the project.

I also like to thank my colleagues and friends for their constructive suggestions and encouragement in the research period. I had an amazing brainstorming while implementing the project with help of everyone.

Finally, I thank all those whose names may not be mentioned here but have supported me.

Place: Delhi

Date: May 2026

Udeesha Gaur

(24/PES/24)

MTech (Power Electronics and Systems)

ABSTRACT

The increase of electric vehicles has led in high demand for efficient and reliable power electronic converters. This work is dedicated to the analysis and control of two advanced converter topologies: the T-type Dual Active Bridge converter and the Ćuk Power Factor Correction (PFC) converter. The Ćuk PFC converter is used for power quality enhancement, current ripple reduction and high power factor maintenance, whereas the T-type Dual active bridge converter is studied for effective bi-directional power transfer, reduced switching stress and improved voltage regulation. Both converters are modelled and simulated in open-loop and closed-loop operation using MATLAB. Simulation results help us to give a better understanding of how both converters are working, their performance and efficiency.

TABLE OF CONTENTS

Acknowledgement (i)
Table of Contents (ii)
List of Figures (iii)
List of Symbols and Abbreviations (iv)

Chapter 1: Introduction 1
1.1 Introduction 1
1.1.1 Introduction to Electric Vehicles 2
1.1.2 Role of Power Electronics in Electric Vehicles 3
1.1.3 The Need for Better Converters 3
1.2 The Dual Active Bridge Converter 4
1.3 The Cuk-PFC Converter 4
1.4 Motivation of the Work 5
1.5 Objectives of the Work 5
1.6 Scope of the Work 5
1.7 Organisation of the Thesis 6

Chapter 2: Literature Review 7
2.1 Introduction 7
2.2 Power Converters in Electric Vehicle Systems 7
2.3 EV Charging Infrastructure in India 8
2.4 Two-Stage and Single-Stage Converter Architectures 9
Two-Stage Architecture 9
Single-Stage Architecture 9
2.5 Comparison of AC and DC Connected EV Charging Architecture 9
2.6 Classification of EV Chargers 10
2.7 Charging Levels 10
2.8 On-board and Off-board Chargers 11
2.9 AC-DC Converter Topologies 11
2.10 Isolated DC-DC Converter Topologies 12
2.11 T-Type Dual active bridge Converter Research 12
2.12 Power Factor Correction (PFC) Research 12
2.14 Summary 13

Chapter 3: Fundamentals of Power Electronic Converters 14
3.1 Introduction 14
3.2 Classification of Power Electronic Converters 14
3.2.1 AC to DC Converter (Rectifier) 15

3.2.4 AC to AC Converter 15
3.3 Power Semiconductor Devices 15
3.4 Switching Techniques in Power Electronic Converters 16
3.5 Pulse Width Modulation (PWM) 17
3.6 Power Quality and Harmonics 17
3.7 Dual Active Bridge (Dual active bridge) Converter 18
3.8 Cuk Converter and Power Factor Correction 18
3.9 Applications of Power Electronic Converters in EVs 19
3.10 Summary 19
Chapter 4: T-Type Dual Active Bridge Converter 21
4.1 Introduction 21
4.2 Comparison of Conventional Dual active bridge and T-Type Dual active bridge 22
4.3 Importance of Dual active bridge converter 23
4.4 Modulation Techniques 24
4.5 Discussion of SPS and Dual Phase Shifting Modulation 25
4.5.1 SPS Modulation Scheme 25
4.5.2 Dual Phase Shifting Modulation Scheme 25
4.6 T-Type Dual active bridge Converter Working and Control 26
4.7 State-Space Modelling 27
4.7.1 Switching Functions and State Equations 27
4.7.2 Generalised Average Model (GAM) 27
4.7.3 Fourier Coefficients of Switching Functions 28
4.7.4 State-Space Form 29
4.7.5 Small-Signal Modelling 30
4.7.6 Closed-Loop System 31
4.8 Simulation Parameters and Results 32
4.8.1 Open-Loop T-Type Dual Active Bridge Converter 32
4.8.2 Closed-Loop T-Type Dual Active Bridge Converter 33
4.9 Conclusion 35
Chapter 5: Cuk Converter and PFC 37
5.1 Introduction 37
5.2 Overview of Power Factor Correction 37
5.3 Conventional PFC Techniques 38
5.4 Advantages of Cuk Converter 39
5.5 Working of Cuk Converter 39
5.5.1 Mode 1: Switch ON, Diode OFF 39
5.5.2 Mode 2: Switch OFF, Diode ON 41

5.6 State-Space Average Model of Cuk Converter 42
5.6.1 Perturbation and Linearisation 42
5.7 Design of Open-Loop Cuk Converter 42
5.8 Closed-Loop Cuk-PFC 44
5.9 Cuk-PFC Component Design 46
5.10 Conclusion 49
6. Conclusion and future scope 50
----- References

LIST OF FIGURES

Figure 2.1 EV sales and stock
Figure 2.2 EV Charging Structure
Figure 3.1 Classification of power converter types Zero Voltage Switching and Zero Current Switching Stress Profiles with Associated Losses
Figure 3.2 Pulse Width Modulation Zero Voltage Switching and Zero Current Switching Stress Profiles with Associated Losses
Figure 3.3 Pulse Width Modulation
Figure 4.1 Power Flow
Figure 4.2 Dual active bridge converter
Figure 4.3 T-Type Dual active bridge converter
Figure 4.4 Types of Modulation
Figure 4.5 Schematic of T-Type Dual Active Bridge Converter
Figure 4.6 Closed-Loop T-Type Dual Active Bridge with Controller
Figure 4.7 Open-Loop Simulations: Primary Voltage, Transformer Primary Voltage, Inductor Current and Secondary Voltage
Figure 4.8 Open-Loop: input and output voltage and output current
Figure 4.9 Closed-Loop - (i) Input Current; (ii) Input Voltage
Figure 4.10 Closed-Loop - MOSFET Voltage Waveforms: (i) MOS Ap; (ii) MOS Bp; (iii) MOS A; (iv) MOS B
Figure 4.11 Closed-Loop - (i) Primary Voltage Vp; (ii) Transformer- Side Primary Voltage; (iii) Impedance Voltage Drop; (iv) Inductor Current
Figure 4.12 Closed-Loop, Output Current and Voltage
Figure 5.1 Mode 1 Circuit Diagram
Figure 5.2 Mode 2 Circuit Diagram
Figure 5.3 Configuration of Cuk-PFC Converter with Control Loop
Figure 5.4 Open-Loop Cuk: I_l vs Time
Figure 5.5 Open-Loop Cuk: I_l vs Time
Figure 5.6 Open-Loop Cuk: Io vs Time
Figure 5.7 Open-Loop Cuk: Vo vs Time
Figure 5.8 Closed-Loop Cuk-PFC: I_l ,Vs , Vo, Io vs Time

LIST OF TABLES

Table 2.1 National Status of EV Charging Infrastructure in India

Table 2.2 Comparison Between DC and AC Bus Architecture

Table 2.3 Classification of EV Chargers

Table 2.4 Charging Classification Based on Levels

Table 2.5 Comparison of On-board and Off-board Chargers

Table 2.6 Comparison of AC-DC Converter Topologies

Table 2.7 Isolated DC-DC Converter Topologies

Table 2.8 Comparison of Modulation Techniques for Dual Active Bridge Converter

Table 4.1 Comparison of Conventional Dual active bridge and T-Type Dual active bridge Converter

Table 4.2 Comparison of Dual Active Bridge with Other Isolated Converter Topologies

Table 4.3 Open-Loop T-Type Dual Active Bridge Simulation Parameters

Table 4.4 Closed-Loop T-Type Dual Active Bridge Simulation Parameters

Table 5.1 Comparison of Active PFC and Passive PFC

Table 5.2 Open-Loop Cuk Converter Parameters

Table 5.3 Closed-Loop Cuk-PFC Parameters

LIST OF SYMBOLS AND ABBREVIATIONS

L	— Inductance (H)
C	— Capacitance (F)
n	— Transformer turns ratio (N1:N2)
δ	— Phase-shift angle (radians)
d_1, d_2	— Inner and outer phase-shift duty ratios
V_i, V_0	— Input and output DC voltages (V)
I_L	— Inductor current (A)
fs	— Switching frequency (Hz)
D	— Duty cycle
P	— Power (W)
pf	— Power factor
ωs	— Switching angular frequency (rad/s)

CHAPTER 1:

INTRODUCTION

1.1 Introduction

The fast-growing technology surrounds renewable energy ever more than non renwable . so electric vehicles (EVs), renewable energy systems, and modern electronic devices have increased the demand for efficient power conversion systems. Power electronic converters are important for controlling and converting electrical energy from one form to another and have inherent features of high efficiency, reliability and power density.

It's better to have bidirectional with the help of a high-frequency transformer for battery charging and many other applications. The efficiency of the vehicle depends upon the converter, losses and power quality of the converters being used in the vehicle. Hence, now advanced converter topologies are being developed to reduce loss or increase efficiency, such that it doesn't defeat the main purpose. The general purpose of building an EV is for better efficiency, less use of fuel, less pollution, cleaner air and less noise pollution.

One of the advanced converters, the Dual Active Bridge, is grabbing a lot of attention due to its advantages over the other converters used for electric vehicle charging. its advantageous due to its bidirectional nature, isolation due to the presence of a transformer, high power density and its soft switching, due to which losses are less. A topology is a dual active bridge, is comparatively is comparatively more famous which is T-Type dual active bridge converter, due to reduced losses, better efficiency, and low conduction losses, making this type more attractive for electric vehicles.

Another major concern in power is its power factor. A low power factor shows that the power transferred or consumed is not clean. High power factor ~.9 is very accurate and that means real power is more, i.e., production of harmonics is very low, which

decreases total harmonic distortion. In AC systems. These harmonics are introduced into power systems due to the presence of non-linear loads which inject harmonics into the system, resulting into low power factor. The Cuk-PFC converter is very popular since it has continuous input and output current with reduced fluctuations.

The thesis is focused on performance analysis of the T-Type Dual Active Bridge converter and the Cuk-PFC converter for electric vehicle applications. This thesis discusses the operation of both the converters individually and the controlling techniques for the smooth operation of converters, yielding good efficiency and reduced losses with the help of simulation in MATLAB. The study discusses the operating principles, control techniques, design analysis, simulation modelling, and performance evaluation of both converters. quality.

1.1.1 Introduction to Electric Vehicles

Electric vehicles are vehicles that are powered by electricity rather than traditional fuels. EVs use rechargeable batteries as their main source of energy and electric motors for propulsion.. Due to increasing environmental concerns, depletion of fossil fuels, and stringent emission regulations, electric vehicles are becoming a major alternative to internal combustion engine vehicles.

Electric vehicles offer several advantages:

- Reduced greenhouse gas emissions
- High energy efficiency
- Low operating cost
- Reduced maintenance requirements
- Quiet operation

Environmental concerns, depletion of fossil fuels and stringent emission regulations are pushing the shift towards electric vehicles as a major alternative to internal combustion engine vehicles.

The main components of an electric vehicle consist of: battery pack, electric motor, power electronic converters, battery management system and charging system. Power electronic converters connect the battery, the motor and the charging system. So, to improve the performance and life of EV batteries, the efficient operation of the converter is necessary.

1.1.2 Role of Power Electronics in Electric Vehicles

While the battery is the heart of an electric vehicle, power electronics are its circulatory system. Every energy transfer in an EV, whether from the grid to the battery, from the battery to the motor, or back from the motor to the battery during regenerative braking, passes through a power converter. These converters must operate over a wide range of voltage and current, and efficiently over a variety of load conditions, and reliably over hundreds of thousands of kilometres and many years of service.

In EV applications, power converters are used for battery charging and discharging, DC-DC voltage conversion between different system buses, motor drive control, regenerative braking energy recovery, and grid interfacing for Vehicle-to-Grid (V2G) operations. These tasks require different performance characteristics, and the converter topology can have a profound effect on the overall system.

1.1.3 The Need for Better Converters

Traditional converter topologies are well proven and reliable but cannot fulfill the requirements of high-performance EVs. The large losses in conventional switches at the high switching frequencies needed for compact and light weight designs are caused by the overlap of voltage and current during each transition. These switching losses produce heat, lower efficiency and require larger cooling systems, which is contrary to the goal of creating smaller, lighter and more efficient vehicles.

Another problem is power quality. The spread of EV chargers can cause significant harmonic distortion on the power grid, which can affect the quality of the power grid, lead to an increase in losses in the distribution networks, and pose problems for other equipment connected to the grid. Therefore, converters with good power factor correction characteristics are not only a nice feature, but an increasingly important requirement for grid-connected EV charging systems .

These limitations have been precisely addressed by the development of advanced topologies such as the T-Type Dual active bridge converter and the Cuk-PFC converter, and their performance in realistic EV scenarios is the aim of thesis.

1.2 The Dual Active Bridge Converter

The Dual Active Bridge converter is one of the most studied isolated bidirectional DC-DC converter topologies during the last two decades. The idea is quite simple. Two active full-bridge circuits are connected through a high-frequency transformer [1], [2]. The transformer leakage inductance is the main element for energy transfer. The converter can precisely control the power transferred and its direction by controlling the phase shift between the switching patterns of the two bridges.

The combination of galvanic isolation, bidirectional power flow, soft-switching capability, high power density and inherent scalability makes the Dual active bridge a great fit for EV charging applications. The T-Type variant takes it one step further by replacing the standard two-level bridge structure with a three-level T-Type topology. This helps to reduce stress on switches, losses, and increased efficiency.

1.3 The Cuk-PFC Converter

Power factor is the ratio of real power to apparent power. A poor factor means the power supplies is useless or noisy. Technically, the total harmonic distortion is high due to the presence of nonlinear loads. Power factor is the ratio of real power consumed to apparent power drawn from the supply.

The Cuk converter is a non-isolated DC-DC conveter because of its ability to both step up and step down the voltage and its continuous current in both the input and output. This continuous-current characteristic gives it a natural advantage in power factor correction duty over topologies such as the boost converter, which has a discontinuous input current that needs to be actively shaped to have good power factor. The Cuk-PFC converter provides low input current ripple, reduced EMI and improved harmonic performance – all useful properties for an EV charger front end.

1.4 Motivation of the Work

The work presented in this thesis has five main goals. First to build the code on both the type of type of converters. Secondly, to produce a generalised averaging model. This averaging will provide a transfer function that helps to regulate the current and voltage needed using control.

This thesis includes only analysis and simulation, and not the Hardware implementation, but is important. Both converter simulations are in open loop as well as closed loop.

1.5 Objectives of the Work

The aim of the thesis:

1. Analyses of T-Type Dual active bridge and Cuk-PFC converters.
2. Check converter performance for EV.
3. To suppress switching losses and increase efficiency.
4. To improve power factor as well as reduce harmonics.
5. Produce MATLAB models of t-dab and cukpfc.

1.6 Scope of the Work

In this thesis the theoretical analysis, the mathematical modelling and the MATLAB/Simulink simulation of the T-Type Dual active bridge converter and the Cuk-PFC converter are presented. The scope covers steady-state and transient performance analysis in open-loop and closed-loop conditions. Hardware implementation is not considered in this work and is a future direction.

1.7 Organisation of the Thesis

This thesis has 6 chapters starting from an introduction about the EV and how to increase its efficiency. To increase efficiency, we need highly efficient converters. Then there is the classification of converters and uses of converters. In further chapters, we have an isolated t type Dual active bridge converter and its performance at the output. Further, we have discussed the importance of CUK- PFC converter and discussed about the operation, analysis and performance of CUK-OPFC converters along with its modelling. At the end, we have jotted down the future scope of the converters in EV withstand.

CHAPTER 2:

LITERATURE REVIEW

2.1 Introduction

Power electronic converters are important components in electric vehicle applications as they provide efficient power conversion, battery charging, voltage regulation and energy management. Researchers have focused on the development of advanced converter topologies which offer better efficiency, lower switching losses, high power density and better power quality. This chapter reviews the existing work on the Dual Active Bridge (Dual active bridge) converters, T-Type Dual active bridge converters, Power Factor Correction (PFC) techniques and Cuk-PFC converters used in electric vehicle systems. Power electronic converters have been studied extensively over the last decades, but the advent of electric vehicles as a mainstream transportation technology has added a new urgency to this field. The specific requirements of EV systems: high efficiency over wide operating ranges, bidirectional power flow, galvanic isolation, compact form factor and excellent power quality, have pushed the converter designers to their limits and created a rich body of literature which this chapter aims to survey. The review includes general electric vehicle power converter research, development of Dual Active Bridge and T-Type Dual active bridge topologies, power factor correction techniques and Cuk-PFC converter.

2.2 Power Converters in Electric Vehicle Systems

The study drew particular attention to the benefits of advanced control strategies — including Sliding Mode Control and Model Predictive Control — in improving converter performance under varying operating conditions. It has been reported a strong trend towards high gain converters, resonant topologies and isolated soft switched topologies. The authors concluded that the soft-switching converters are especially well-suited to EV applications where efficiency is of prime importance, as they reduce switching losses by ensuring either voltage or current is zero at the moment of switching.

2.3 EV Charging Infrastructure in India

India's electric vehicle industry is growing rapidly thanks to strong government initiatives and increasing public awareness about clean transportation technologies.

The key problem identified is that the development of charging infrastructure is not keeping pace with the rate of EV adoptions.

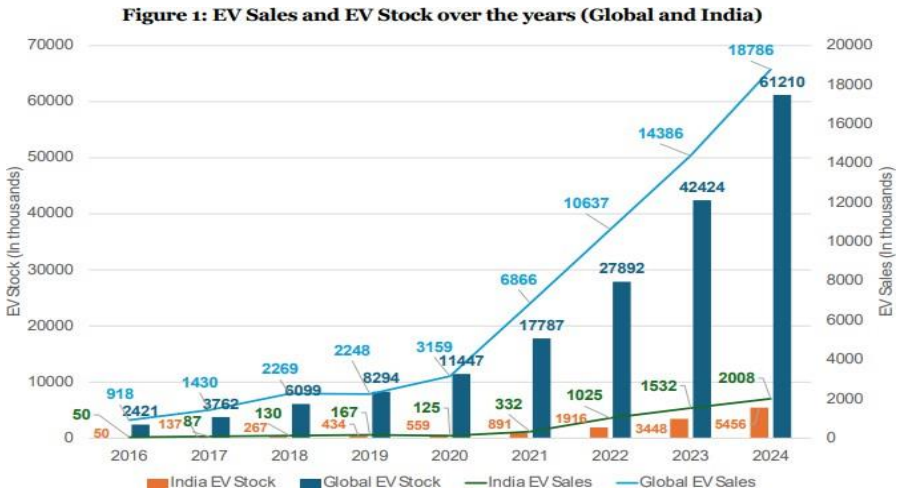

Fig. 2.1: Sales and Stock

Table 2.1: National Status of EV Charging Infrastructure in India

Parameter	Details
Market Growth	Market expected to grow from $3.21B (2022) to $113.99B (2029)
CAGR	66.52%
Government Support	FAME India Scheme, PM-E-DRIVE Scheme
Charging Infrastructure Goal	1.32 million charging stations by 2030
EV Penetration Targets	30% private cars, 70% commercial vehicles
Projected EVs by 2030	80 million EVs
Current Sales Trend	EV sales doubled in 2024–25

2.4 Two-Stage and Single-Stage Converter Architectures

Two-Stage Architecture

In two-stage charging architecture, power conversion occurs at two stages: DC to AC conversion and then followed by DC to DC conversion. The advantages are simple control technique, high reliability, reported efficiency in the range of 98.1% and power density of the order of 3.8kW/L. Limitations include large size and volume. Lower power density and higher cost per kW.

Single-Stage Architecture

The single-stage architecture integrates the AC-DC and DC-DC conversion into one stage. Advantages are small size, no bulky DC-link capacitor, high efficiency (up to 99%) and power density (approx. 7.3 kW/L). Limitations are complex control strategy and sophisticated converterdesign.

2.5 Comparison of AC and DC Connected EV Charging Architecture

Table 2.2: Comparison Between DC and AC Bus Architecture

Criteria	DC Bus Architecture	AC Bus Architecture
Integration of Energy Sources	Easy	Complex
Conversion Stages	Less	More
Efficiency	More	Less
Utility Side Impact	Less	High
AC-DC Rectifier Rating	More	Average
Protection Devices	Sophisticated	Unsophisticated
Control	Simple	Complex
Cost	Less	More

The DC-connected architecture is more efficient and simpler to integrate with renewable energy systems..

2.6 Classification of EV Chargers

EV chargers are classified based on placement, power rating, and direction of power flow.

Table 2.3: Classification of EV Chargers

Based on Placement	Charging Level	Power Rating
On-board charger	Level 1	3.7 KW
On-board charger	Level 2	3.7–22 KW
Off-board charger	Level 3	22–43.5 KW
Off-board DC fast charger	Level 4	Up to 350 KW

Unidirectional chargers are easy to control, cheaper, and cause less battery degradation. Bidirectional chargers allow V2G, V2H and V2L operation but are more complex to control and more expensive.

2.7 Charging Levels

Table 2.4: Charging Classification Based on Levels

Charging Type	Power Level	Charging Time
Level-1 AC Charging	1.44–1.92 kW	11–36 hours
Level-2 AC Charging	3.1–19.2 kW	2–6 hours
Level-3 DC Fast Charging	50–350 kW	<30 minutes
Ultra-Fast DC Charging	400 kW+	≈10 minutes

Fast charging systems can significantly reduce charging time, but also pose greater thermal and grid challenges.

2.8 On-board and Off-board Chargers

Table 2.5: Comparison of On-board and Off-board Chargers

On-board Charger	Off-board Charger
Slow charging	Fast charging
Added weight in EV	No additional EV weight
Lower cost	Higher cost
Minimal battery heating	Battery heating challenges
No burden on grid	May burden grid

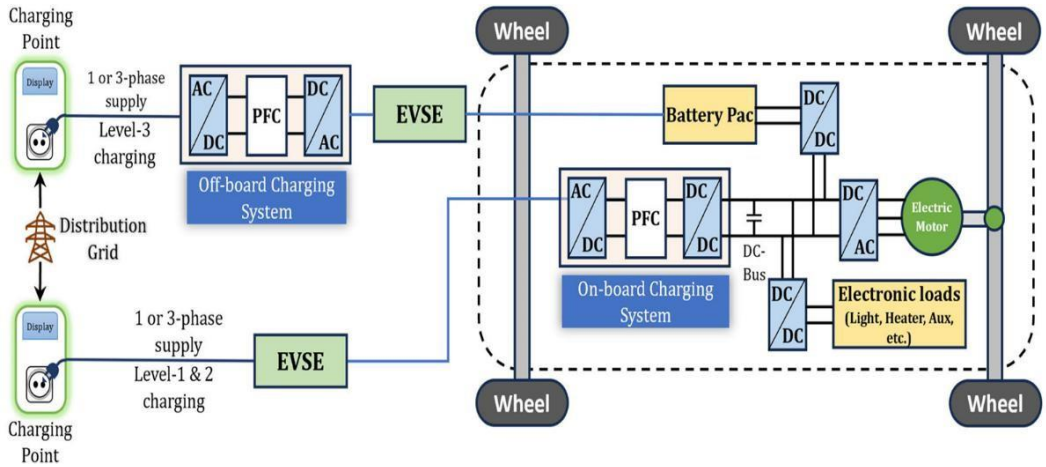

Figure 2.2: On-board and Off-board EV Charging Structure

2.9 AC-DC Converter Topologies

Table 2.6: Comparison of AC-DC Converter Topologies

Topology	Merits	Demerits
PWM Rectifier	Unity PF, low THD, bidirectional	High switching loss
Vienna Rectifier	High efficiency, low THD	Unidirectional
T-Type Converter	High power density, V2G support	Thermal stress
NPC Converter	Lower voltage stress	Voltage balancing issue

2.10 Isolated DC-DC Converter Topologies

Table 2.7: Isolated DC-DC Converter Topologies

Topology	Merits	Demerits
Phase Shift Full Bridge	Zero Voltage Switching operation	Unidirectional
Dual Active Bridge	Bidirectional, soft switching	Complex control
Three-Phase Dual active bridge	High power density	More switches
LLC/CLLC Resonant	Easy soft switching	Limited voltage gain

2.11 T-Type Dual active bridge Converter Research

The T-Type Dual active bridge converter has been paid much research attention as a promising high-performance alternative of traditional Dual active bridge for high-power EV applications. The three-level switching structure of the T-Type bridge reduces the voltage stress on the outer switches to half of that of a standard two-level bridge, which directly reduces switching losses and allows the use of lower-rated — and thus faster-switching — semiconductor devices. The literature on T-Type and Neutral Point Clamped Dual active bridge converters has shown their advantages in terms of switching losses, conduction losses, soft-switching range, thermal performance, electromagnetic interference among others.

Most remarkable is the work where a data-driven modelling and advanced modulation strategies are applied to an NPC-Dual active bridge converter with experimental tests showing peak efficiencies above 98%.

2.12 Power Factor Correction (PFC) Research

Since the 1980s, when switch-mode power supplies became widespread, causing the first large-scale harmonic pollution problems, power factor correction has been an active research area. A detailed review on PFC converter topologies used in EV applications was presented, comparing the harmonic performance, efficiency and power density of unidirectional and bidirectional structures. The review covered boost PFC, buck-boost PFC, Proportional Integral PFC and Cuk-PFC converters etc.

The basic problem in PFC design is to force the input current waveform to follow the sinusoidal input voltage as close as possible to achieve a power factor close to unity and to minimize harmonic content. Different topologies achieve this goal with different trade-offs between complexity, efficiency and performance under varying load conditions. More recent research has confirmed the appropriateness of Cuk-PFC converters for on-board battery charging systems, especially in the scenarios where electromagnetic compatibility is an issue [5].

2.14 Summary

This review has surveyed the research landscape for EV power converters, with particular attention to Dual active bridge and T-Type Dual active bridge topologies, PFC techniques, and the Cuk-PFC converter. Several conclusions emerge clearly. First, isolated bidirectional converters — and the Dual active bridge family in particular — are the preferred choice for EV battery charging interfaces because of their combination of isolation, bidirectional capability, and soft-switching efficiency. Second, T-Type and other multilevel variants of the Dual active bridge offer meaningful efficiency advantages over the conventional two-level topology, especially at the high power levels required for fast charging. Third, the Cuk-PFC converter's continuous-current characteristics make it an excellent choice for the AC-DC front end of an EV charger, where power quality is critical. This thesis builds on these findings by providing a detailed simulation-based performance of both topologies.

CHAPTER 3:

FUNDAMENTALS OF POWER ELECTRONIC CONVERTERS

3.1 Introduction

To understand the T-type Dual active bridge and Cuk-PFC converters, a good knowledge in the field of power electronics is needed. This chapter lays the groundwork with chapters on classification of converters, the semiconductor devices forming their switching elements, the switching techniques that control their operation, the PWM techniques used for their control and the power quality issues that are the motivation for a large part of the research in this thesis. If you are already familiar with these basics, you may wish to skip forward to Chapter 4 where the T-Type Dual active bridge analysis begins.

The difference between power electronics and linear electronics is that the semiconductor devices act as switches - either fully on or fully off - instead of a continuously conducting linear region. This mode of operation by switching enables power transfer with very low loss, since an ideal switch dissipates no power regardless of how much current it carries or voltage it blocks.

3.2 Classification of Power Electronic Converters

We can easily understand the type of converters we often use in power electronics for many applications through the arrow diagram

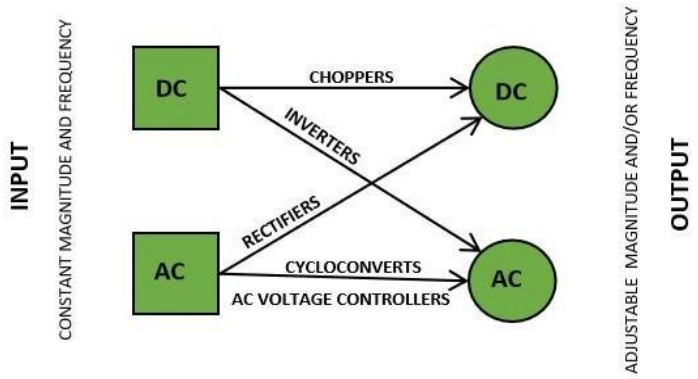

[14]

Figure 3.1: Classification of Power Converter Types

3.2.1 AC to DC Converter (Rectifier)

Is an electrical device which converts AC into DC. Some are uncontrolled rectifiers, like a diode, by using half-bridge or full-bridge rectifiers. Then there are controlled rectifiers that are thyristors (SCR's) . In this, thyristors are controlled by a firing angle. Again, its structure can be a full-wave or a half-wave rectifier. Applications are many, like laptop chargers, TVs, DC alternators, and HVDC for high voltage transfer through large lengths.

3.2.3 DC to DC Converter

DC-DC converters are used to convert one level of DC voltage to another and are widely used in EV charging and battery management systems. These are classified as buck, boost, buck-boost, isolated and non-isolated converters. Isolated converters use high frequency transformers for galvanic isolation and safety. The Dual Active Bridge (Dual active bridge) converter is one of the most popular converters for high power bidirectional EV charging applications.

3.2.4 AC to AC Converter

AC-AC converters are used to change the voltage , frequency or phase of an AC supply without converting it to DC . Typical examples are cycloconverters, matrix converters, and ac voltage regulators. These converters are used in industrial drives and traction applications requiring variable frequency operation. They are less common in EV chargers but do play an important role in motor control applications

3.3 Power Semiconductor Devices

Power diode is an uncontrolled semiconductor device which allows current in only one direction. It is widely used in rectifiers and free wheeling circuits due to its simplicity and high reliability.

MOSFET is a voltage controlled switch device which is known for high switching speed and low switching losses. It has been widely used in high frequency DC-DC converter and EV charging applications.

IGBT is a combination of a MOSFET's high input impedance and a bipolar transistor's high current handling capability. It is widely used in medium and high power converters such as motor drives and traction systems.

SiC MOSFETs are wide band gap semiconductor devices that provide higher efficiency, lower switching losses and higher temperature operation. They are increasingly being used in fast EV chargers and high frequency Dual active bridge converters.

3.4 Switching Techniques in Power Electronic Converters

In hard switching, the semiconductor device is switched ON and OFF with voltage and current both applied across it. This results in large switching losses because of the overlap of voltage and current during switching. The hard switching creates electromagnetic interference (EMI) and also heats the devices. It is simple to implement, but at high switching frequencies it becomes inefficient.Soft switching allows for zero voltage or zero current during switching transitions, thereby reducing switching losses. The two main techniques are Zero Voltage Switching (Zero Voltage Switching) and Zero Current Switching (Zero Current Switching). Such techniques improve efficiency, reduce thermal stress and minimize EMI. In Dual active bridge converters, Zero Voltage Switching operation is often implemented for high-frequency applications such as EV charging..

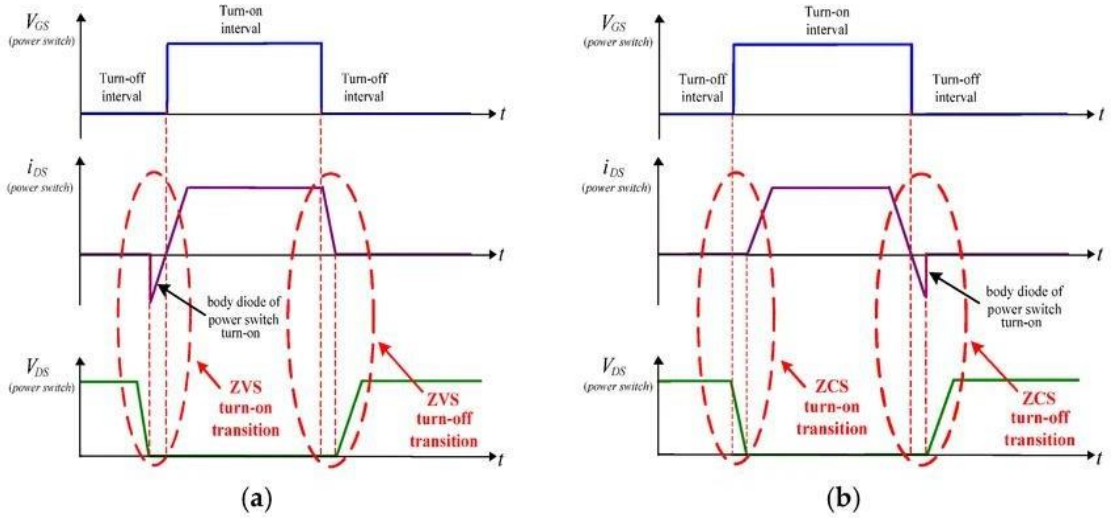

Fig. 3.2: Zero Voltage Switching and Zero Current Switching Stress Profiles with Associated Losses

3.5 Pulse Width Modulation (PWM)

Pulse Width Modulation (PWM) is a technique of control used for controlling the output voltage and current of the converter. It operates by changing the duty cycle of the switching pulses at a constant switching frequency. PWM provides accurate voltage regulation, lower harmonic distortion, higher efficiency. It is widely used in inverters, rectifiers and DC-DC converters.

Different from traditional PWM converters, the Dual active bridge converter uses phase shift modulation between the primary and secondary bridges for the power transfer control. The power flow direction and magnitude depend upon the phase difference of the bridge voltages. This technique can realize bi-directional power transfer and soft-switching operation. It is very suitable for stand-alone high power EV charging systems.

The Single Phase Shift modulation uses a single phase-shift angle to regulate the power transfer between the two bridges. It is simple to implement and widely used in traditional Dual active bridge converters. However, SPS results in increased circulating currentwith high RMS current.

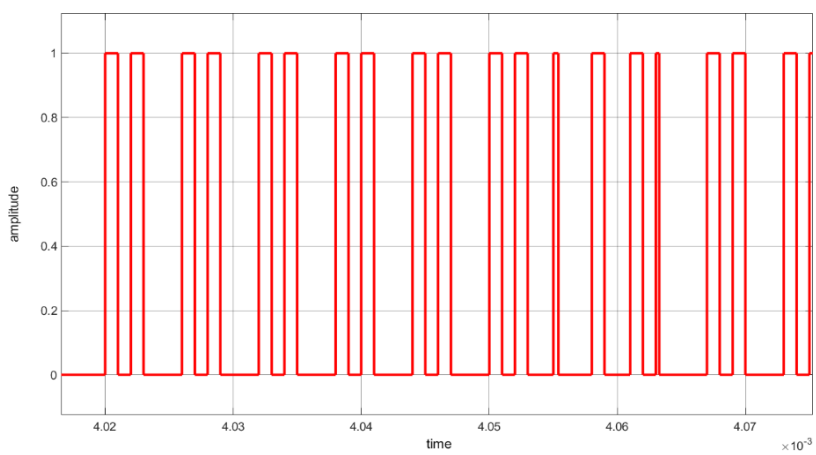

Fig. 3.3: PULSE WIDTH MODULATION

3.6 Power Quality and Harmonics

Power quality refers to the degree to which the voltage and current waveforms in a power system conform to their ideal sinusoidal form. Harmonics — frequency components at integer multiples of the fundamental frequency — are introduced into the system

whenever non-linear loads, including switch-mode power supplies and chargers, draw non-sinusoidal currents from a sinusoidal supply. These harmonics cause a range of problems: increased losses in distribution wiring and transformers, overheating of neutral conductors, interference with sensitive electronic equipment, and degradation of the power factor

Power factor is the ratio of real power to apparent power:

$$pf = \frac{P}{S}$$

A power factor of 1 means that all the current drawn from the supply is doing useful work; a lower power factor means some current is merely circulating, doing no useful work but still causing resistive heating in the distribution system. Modern PFC converters are designed to draw current that closely follows the supply voltage, achieving power factors above 0.99 and total harmonic distortion well below the limits imposed by standards such as IEC 61000-3-2.

3.7 Dual Active Bridge (Dual active bridge) Converter

A dual active bridge consists of 2 bridges with a transformer in between them. These are 2 full bridges with controlled switches. We can use MOSFETs, IGBTs, and BJTs, but the characteristics of MOSFETs are the most ideal and least lossy [5].

The dual active bridge topology has been used in:

- EV charging systems
- Renewable energy systems
- Battery energy storage systems
- Smart transformers

Recent research indicates that Dual active bridge converters achieve high efficiency above 97–98% for wide-voltage EV charging applications [4].

3.8 Cuk Converter and Power Factor Correction

The Cuk converter is a DC-DC converter capable of providing both step-up and step-down voltage conversion with continuous input and output currents.

Advantages

- Reduced input current ripple
- Better EMI performance
- Improved power factor
- Continuous current operation

When integrated with power factor correction techniques, the Cuk-PFC converter improves grid current quality, power factor, and harmonic performance, making it suitable for EV charging systems.

3.9 Applications of Power Electronic Converters in EVs

Power electronic converters are widely used in electric vehicle systems for battery charging, motor drive operation, regenerative braking, Vehicle-to-Grid (V2G) operation, and energy management. Modern EV fast chargers require high efficiency, fast charging capability, reduced harmonics, and a compact converter structure.

Research papers show that modular Dual active bridge converters and PFC converters are highly suitable for future EV charging infrastructure because of their scalability and bidirectional operation capability.

3.10 Summary

This chapter has provided the theoretical background necessary for the detailed analysis of the T-Type Dual active bridge and Cuk-PFC converters in the chapters that follow. The key concepts to carry forward are the principles of soft switching (and why the Dual active bridge achieves it), the role of phase-shift modulation in Dual active bridge control, and the importance of continuous input current in achieving good power factor correction. With this foundation in place, the next chapter turns to the T-Type Dual active bridge converter in detail.This chapter has provided the theoretical background necessary for the detailed analysis of the T-Type Dual active bridge and Cuk-PFC converters in the chapters that follow. The key concepts to carry forward are the principles of soft switching (and why the Dual active bridge achieves it), the role of phase-shift modulation in Dual active bridge control, and the importance of continuous input current in achieving good power

factor correction. With this foundation in place, the next chapter turns to the T-Type Dual active bridge converter in detail.

CHAPTER 4:

T-TYPE DUAL ACTIVE BRIDGE CONVERTER

4.1 Introduction

Electric vehicles (EVs) are gaining popularity at an unprecedented rate creating a strong need for efficient and fast charging infrastructure. Battery technology has improved driving range, but charging time is still a major hurdle. The converters in EV charging systems should have good efficiency, small size and reliability [5].

Among the DC-DC converters, the Dual Active Bridge (Dual active bridge) converter is widely used due to its bidirectional operation and high power density. The Dual active bridge DC-DC converters have received great attention in the EV charging and DC grid applications due to their bidirectional power flow capability, galvanic isolation, and high efficiency. These features provide bidirectional energy flow that allows for applications such as regenerative braking and V2G operation [12]. But it suffers from high current stress in different operating conditions. To overcome these problems, advanced converter topologies such as T-type topologies are investigated.

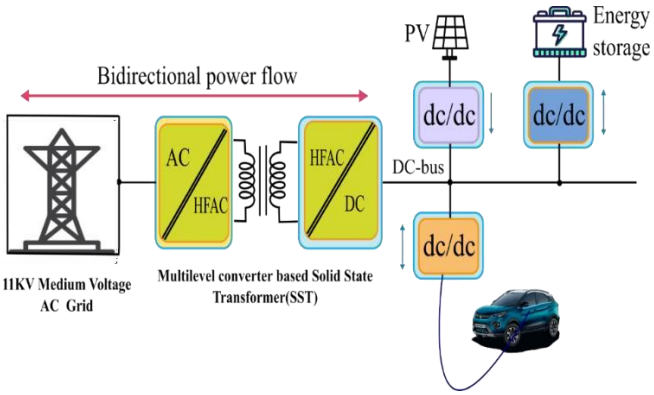

Fig. 4.1 POWER FLOW

In this work, a T-type Dual active bridge converter is investigated with a control strategy based on the Proportional Integral control under the Dual Phase Shifting modulation. The system is modelled using a Generalised Averaging Method (GAM) and the performance is studied for various operating conditions. Simulation results show the stable operation, better voltage regulation and reduction in losses [9].

4.2 Comparison of Conventional Dual active bridge and T-Type Dual Active Bridge

Conventional Dual Active Bridge

The standard Dual Active Bridge converter is composed of two full bridges coupled by a high-frequency transformer. It mainly offers:

• Bidirectional flow of power

• Galvanic isolation

• high power density

But, it has more switching loss and device stresses [4].

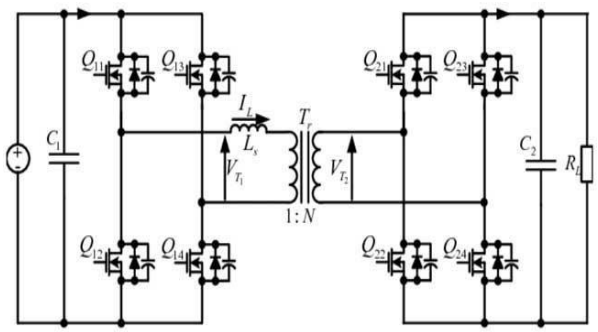

Fig 4.2: Dual active bridge converter **[12]**

T-Type Dual active bridge

The T-Type Dual active bridge is an improved version of the conventional Dual active bridge in which the bridge structure is converted to a T-Type three-level topology which gives [12]:

- Lower switching losses
- Better soft switching
- Improved efficiency and waveform quality

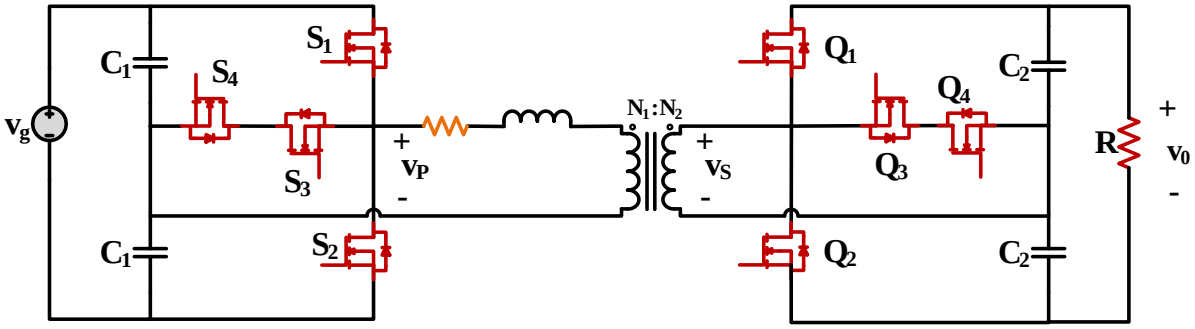

Fig. 4.3: T-TYPE Dual active bridge converter

Table 4.1: Comparison of Conventional Dual active bridge and T-Type Dual active bridge Converter

Parameter	Conventional Dual active bridge	T-Type Dual active bridge
Converter Structure	Two-level full bridge	Three-level T-Type bridge
Voltage Levels	±Vdc	+Vdc/2, 0, −Vdc/2
Switching Loss	Higher	Lower
Voltage Stress on Switches	High	Reduced
Waveform Quality	Moderate	Better
Efficiency	High	Very High
Complexity	Simple	More complex
Harmonics	More	Less
Cost	Lower	Higher

The T-Type Dual active bridge is an improved multilevel form of the conventional Dual active bridge converter. It has lower switching losses, voltage stress, better soft switching and higher efficiency and waveform quality by modifying the bridge structure to a three-level T-type topology [9],[12].

4.3 Importance of Dual active bridge converter

Table 4.2: Comparison of Dual active bridge with Other Isolated Converter Topologies

Feature	Dual active bridge	Flyback/Forward	LLC Resonant	PSFB
Power Flow	Bidirectional	Unidirectional	Bidirectional	Unidirectional
Control Method	Phase-Shift	Duty Cycle (PWM)	Frequency Modulation	Phase-Shift
Soft-Switching	Zero Voltage Switching — wide range	Hard switching (unless modified)	Excellent Zero Voltage Switching+Zero Current Switching	Excellent Zero Voltage Switching (primary)
Ideal Use Case	EV/V2G/Smart transformer	Low-power cost-sensitive adapters	High-efficiency fixed-ratio	High-power unidirectional systems

The Dual Active Bridge (Dual active bridge) converter is characterized by bidirectional power flow, galvanic isolation and symmetrical topology. Standard isolated topologies are generally unidirectional, employing diodes for rectification. In the Dual active bridge, diodes are substituted by active switches on both sides, enabling a smooth flow of energy in either direction[12].

4.4 Modulation Techniques

Table 2.8: Comparison of Modulation Techniques for Dual active bridge Converter

Technique	Complexity	Efficiency	Circulating Current	Zero Voltage Switching Range
SPS	Low	Moderate	High	Limited
Dual Phase Shifting	Medium	High	Reduced	Wider
Triple Phase Shifting	Very High	Very High	Very Low	Widest
EPS	Medium	High	Reduced	Improved

Technique	Complexity	Efficiency	Circulating Current	Zero Voltage Switching Range
PWM	High	High	Moderate	Good
Frequency Modulation	Medium	High	Reduced	Good

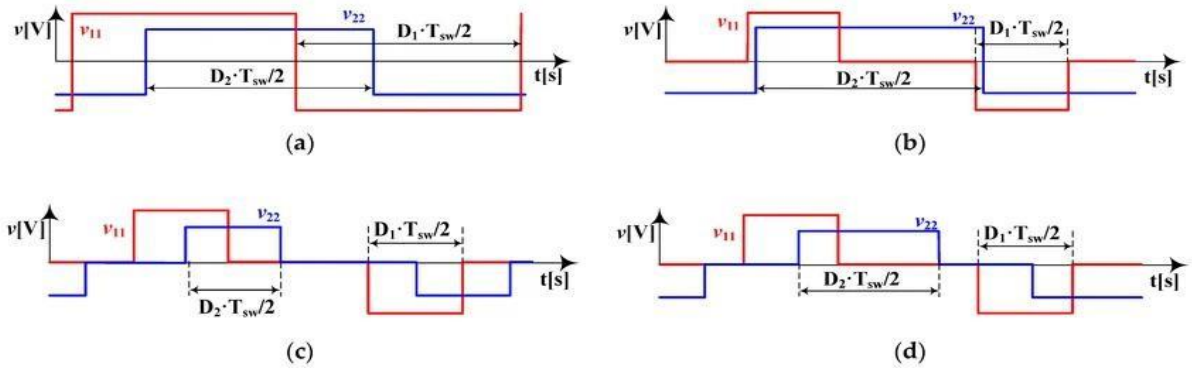

Figure 4.4 : Types of Modulation Applied to Dual active bridge Converter: (a) Phase Shift (SPS); (b) Extended Phase Shift (EPS); (c) Dual Phase Shift (Dual Phase Shifting); (d) Triple Phase Shift (Triple Phase Shifting) [10], [11],[12].

4.5 Discussion of SPS and Dual Phase Shifting Modulation

4.5.1 SPS Modulation Scheme

SPS modulation is the simplest method of controlling the Dual active bridge. Both H-bridges switch with a fixed 50% duty cycle, resulting in high-frequency square-wave voltages V1 and V2 at the transformer terminals. The phase shift between V1 and V2 is used to control the power flow. The sign of the phase shift indicates the direction of power flow. If V1 leads V2, power flows from the primary side to the secondary side.

In Single phase shifting, circulating current is generated due to the fact that the two active bridges do not produce square-wave voltages that are perfectly aligned when in phase-shift operation. Even when lightly loaded, significant amounts of current flow among bridges without transferring useful power. The circulating current mainly increases in light load conditions, small phase-shift angles and voltage mismatch between bridges, which leads to higher RMS current, more conduction and switching losses, transformer heating, decreased efficiency, and large stress on switches.

4.5.2 Dual Phase Shifting Modulation Scheme

Dual Phase Shift (Dual Phase Shifting) control employs two phase-shift variables; D1 (inner phase-shift ratio that specifies the switching durations within a bridge) and D2 (outer phase-shift ratio that specifies the power transfer between primary and secondary). The converter uses this extra control to shape the transformer current better. Dual Phase Shifting reduces the unnecessary overlapping between the bridge voltages by tuning the internal phase shift. This reduces the reactive power circulation through the leakage inductance.

Thus RMS current decreases, conduction losses reduces, switching losses reduces, transformer heating reduces, efficiency improves and Zero Voltage Switching range becomes wider. However, circulating current is not completely eliminated in Dual Phase Shifting due to the energy storage of leakage inductances, imperfect voltage matching, load variations and non-ideal switching conditions.

4.6 T-Type Dual active bridge Converter Working and Control

The T-Type Dual active bridge converter comprises two full bridges with two auxiliary switches and a high frequency transformer (HFT) with leakage inductance L_l for galvanic isolation. The DC voltages at the input and output are V_i and V_o respectively. The DC link link capacitors C_i and C_o are assumed to be large enough to make the input and output voltages have less ripple.

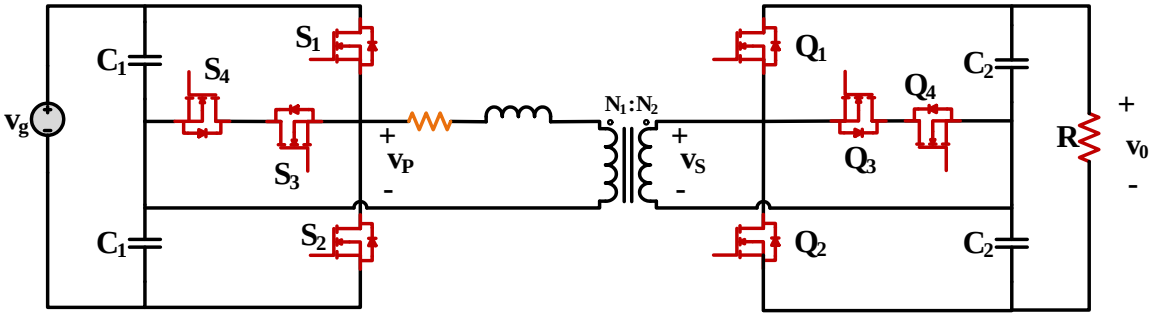

Fig. 4.6: Schematic of T-Type Dual active bridge Converter

The high frequency transformer is utilized for power transfer between two DC sources by controlling the switching phase angle of the bridges. The primary and secondary T-bridges produce the three level high frequency voltage waveforms and the difference of the waveforms results in the flow of current through the leakage inductance. The basic equations of converter operation are:

$$n = \frac{N_1}{N_2} \tag{4.1}$$

$$V_L = V_p - nV_s \tag{4.2}$$

$$P = \left(\frac{nV_{iV_o}}{1}\omega L\right)\delta\ \left(1 - \frac{\delta}{\pi}\right) \tag{4.3}$$

Maximum power transfer condition: δ = π/2

$$C\ \left(\frac{aV_{out}}{dt}\right) = i_L - i_o \tag{4.4}$$

4.7 State-Space Modelling

4.7.1 Switching Functions and State Equations

The switching functions S1(τ, d) and S2(τ, d) describe the three-level bridge output voltages. With state variables I_L (inductor current) and V_o (output voltage), the dynamic equations of the converter are:

$$S_1(t,d) = \{1;\ 0 < t < d_1T_{hs}\ 0;\ d_1T_{hs} < t < T_{hs}\ \ -1;\ T_{hs} < t < (1+d_1)T_{hs}\ or\ (1+d_1)T_{hs} < t < 2T_{hs} \tag{4.6}$$

[12]

$$S_2(t,d) = \{1;\ d_2T_{hs} < t < (d_1+d_2)T_{hs}\ 0;\ (d_1+d_2)T_{hs} < t < (1+d_2)T_{hs}\ \ -1;\ (1+d_2)T_{hs} < t < (1+d_1+d_2)T_{hs}\ \ or\ (1+d_1+d_2)T_{hs} < t < (2+d_2)T_{hs} \tag{4.7}$$

[12]

4.7.2 Generalised Average Model (GAM)

The full harmonic expansion of the state equations is performed by means of the Generalised State Space Averaging (GSSA) method. If we assume that $\langle v_i \rangle = V_i$ and that there are no harmonics on the input voltages, then the simplified harmonic equations become

Full harmonic expansion before simplification:

$$\frac{d}{dt}\langle i_L\rangle_0 = -\frac{R}{L}\langle i_L\rangle_0 + \frac{1}{2L}[\langle S_1\rangle_0\langle v_i\rangle_0 + 2\langle S_1\rangle_{1R}\langle v_i\rangle_{1R} + 2\langle S_1\rangle_{1i}\langle v_i\rangle_{1i} - n(\langle S_2\rangle_0\langle v_0\rangle_0 + 2\langle S_2\rangle_{1R}\langle v_o\rangle_{1R} + 2\langle S_2\rangle_{1i}\langle v_o\rangle_{1i})]$$

$$\frac{d}{dt}\langle i_L\rangle_{1R} = -\frac{R}{L}\langle i_L\rangle_{1R} + \omega_s\langle i_L\rangle_{1i} + \frac{1}{2L}[\langle S_1\rangle_0\langle v_i\rangle_{1R} + \langle S_1\rangle_{1R}\langle v_i\rangle_0] - \frac{n}{2L}[\langle S_2\rangle_0\langle v_0\rangle_{1R} + \langle S_2\rangle_{1R}\langle v_0\rangle_0]$$

$$\frac{d}{dt}\langle i_L\rangle_{1i} = -\frac{R}{L}\langle i_L\rangle_{1i} - \omega_s\langle i_L\rangle_{1R} + \frac{1}{2L}[\langle S_1\rangle_0\langle v_i\rangle_{1i} + \langle S_1\rangle_{1i}\langle v_i\rangle_0] - \frac{n}{2L}[\langle S_2\rangle_0\langle v_0\rangle_{1i} + \langle S_2\rangle_{1i}\langle v_0\rangle_0]$$

$$\frac{d}{dt}\langle v_0\rangle_0 = -\frac{1}{RC_0}\langle v_0\rangle_0 + \frac{n}{C_0}[\langle S_2\rangle_0\langle i_L\rangle_0 + 2\langle S_2\rangle_{1R}\langle i_L\rangle_{1R} + 2\langle S_2\rangle_{1i}\langle i_L\rangle_{1i}]$$

$$\frac{d}{dt}\langle v_0\rangle_{1R} = -\frac{1}{RC_0}\langle v_0\rangle_{1R} + \omega_s\langle v_0\rangle_{1i} + \frac{n}{C_0}[\langle S_2\rangle_0\langle i_L\rangle_{1R} + \langle S_2\rangle_{1R}\langle i_L\rangle_0]$$

$$\frac{d}{dt}\langle v_0\rangle_{1i} = -\frac{1}{RC_0}\langle v_0\rangle_{1i} - \omega_s\langle v_0\rangle_{1R} + \frac{n}{C_0}[\langle S_2\rangle_0\langle i_L\rangle_{1i} + \langle S_2\rangle_{1i}\langle i_L\rangle_0]$$

...(4.8)[12]

Assumptions:

$$< v_i >= V_i; \quad < v_{i1R} > = < v_{i1i} > = 0; \quad < S_{10} > = < S_{20} > = 0$$

The input voltage, Vi, changes slowly compared to the dynamics of the Dual active bridge output voltage and inductor current.

Simplified Harmonic Equations:

$$\frac{d}{dt}\langle i_L\rangle_0 = -\frac{R}{L}\langle i_L\rangle_0 + \frac{n}{L}[\langle S_2\rangle_{1R}\langle v_o\rangle_{1R} + \langle S_2\rangle_{1i}\langle v_o\rangle_{1i}]$$

$$\frac{d}{dt}\langle i_L\rangle_{1R} = -\frac{R}{L}\langle i_L\rangle_{1R} + \omega_s\langle i_L\rangle_{1i} + \frac{1}{2L}[\langle S_1\rangle_{1R}\langle v_i\rangle_0 - n\langle S_2\rangle_{1R}\langle v_0\rangle_0]$$

$$\frac{d}{dt}\langle i_L\rangle_{1i} = -\frac{R}{L}\langle i_L\rangle_{1i} - \omega_s\langle i_L\rangle_{1R} + \frac{1}{2L}[\langle S_1\rangle_{1i}\langle v_i\rangle_0 - n\langle S_2\rangle_{1i}\langle v_0\rangle_0]$$

$$\frac{d}{dt}\langle v_0\rangle_0 = -\frac{1}{RC_0}\langle v_0\rangle_0 + \frac{2n}{C_0}[\langle S_2\rangle_{1R}\langle i_L\rangle_{1R} + \langle S_2\rangle_{1i}\langle i_L\rangle_{1i}]$$

$$\frac{d}{dt}\langle v_0\rangle_{1R} = -\frac{1}{RC_0}\langle v_0\rangle_{1R} + \omega_s\langle v_0\rangle_{1i} + \frac{n}{C_0}[\langle S_2\rangle_{1R}\langle i_L\rangle_0]$$

$$\frac{d}{dt}\langle v_0\rangle_{1i} = -\frac{1}{RC_0}\langle v_0\rangle_{1i} - \omega_s\langle v_0\rangle_{1R} + \frac{n}{C_0}[\langle S_2\rangle_{1i}\langle i_L\rangle_0]$$

....(4.9)[12]

4.7.3 Fourier Coefficients of Switching Functions

The Fourier coefficients of the switching functions S1 and S2 are:

$$S_{1R}(D) = sin\ sin\ (d_1\pi) \tag{4.10a}$$

$$S_{1i}(D) = -\frac{2sin^2\left(\frac{d_1\pi}{2}\right)}{\pi} \tag{4.10b}$$

$$< S_2 >_{1R}\ (D) = -\frac{1}{\pi}[sin\ sin\ (d_2\pi)\ -sin\ sin\ ((d_1 + d_2)\pi)\ ] \tag{4.10c}$$

$$< S_2 >_{1i}\ (D) = -\frac{1}{\pi}[cos\ cos\ (d_2\pi)\ -cos\ cos\ ((d_1 + d_2)\pi)\ ] \tag{4.10d}$$

4.7.4 State-Space Form

The state vector and input are defined as:

$$x = [\langle i_L\rangle_0 \quad \langle i_L\rangle_{1R} \quad \langle i_L\rangle_{1i} \quad \langle v_0\rangle_0 \quad \langle v_0\rangle_{1R} \quad \langle v_0\rangle_{1i}]^T, \quad u = \langle v_i\rangle_0 \tag{4.11}$$

$$\dot{x} = A(D)\,x + B(D)\,u \tag{4.12}$$

The 6×6 system matrix A(D) contains duty-dependent entries derived from the Fourier coefficients. The key off-diagonal elements are:

The system matrix A(D) is 6×6 system matrix and its entries depend on the duty and come from the Fourier coefficients. The main off-diagonal elements are:

The 6×6 state matrix with duty-dependent entries:

$$A(D) = [-\frac{R}{L}\ 0\ 0\ 0\ \alpha_{14}\ \alpha_{15}\ 0\ -\frac{R}{L}\ \omega_s\ \alpha_{24}\ 0\ 0\ 0\ -\omega_s$$
$$-\frac{R}{L}\ \alpha_{34}\ 0\ 0\ 0\ \alpha_{41}\ \alpha_{42}\ -\frac{1}{RC_0}\ 0\ 0\ \alpha_{51}\ 0\ 0\ 0$$
$$-\frac{1}{RC_0}\ \omega_s\ \alpha_{61}\ 0\ 0\ 0\ -\omega_s\ -\frac{1}{RC_0}\ ] \tag{4.13}$$

[12]

Coefficient Definitions —

$$\alpha_{14} = -\frac{n}{L\pi}(sind_2\pi - sin(d_1 + d_2)\pi) \quad (4.14a)$$

$$\alpha_{15} = -\frac{n}{L\pi}(cosd_2\pi - cos(d_1 + d_2)\pi) \quad (4.14b)$$

$$\alpha_{24} = \frac{n}{2L\pi}(sind_2\pi - sin(d_1 + d_2)\pi) \quad (4.14c)$$

$$\alpha_{34} = \frac{n}{2L\pi}(cosd_2\pi - cos(d_1 + d_2)\pi) \quad (4.14d)$$

$$\alpha_{41} = -\frac{2n}{C_0\pi}(sind_2\pi - sin(d_1 + d_2)\pi) \quad (4.14e)$$

$$\alpha_{42} = -\frac{2n}{C_0\pi}(cosd_2\pi - cos(d_1 + d_2)\pi) \quad (4.14f)$$

$$\alpha_{51} = -\frac{n}{C_0\pi}(sind_2\pi - sin(d_1 + d_2)\pi) \quad (4.14g)$$

$$\alpha_{61} = -\frac{n}{C_0\pi}(cosd_2\pi - cos(d_1 + d_2)\pi) \quad (4.14h)[12]$$

A-matrix element expressions & numerical values

Symbol	Expression	Value
A_{11}	$-1/(R \cdot C_0)$	-100.0000
A_{12}	$(2n/C_0\pi)\cdot[\sin((D_1+D_2)\pi) - \sin(D_2\pi)]$	0.0000
A_{13}	$(2n/C_0\pi)\cdot[\cos((D_1+D_2)\pi) - \cos(D_2\pi)]$	-6564.8371
A_{21}	$-(n/2L\pi)\cdot[\sin((D_1+D_2)\pi) - \sin(D_2\pi)]$	0.0000
A_{22}	$-R/L$	$-3{,}134{,}796.24$
A_{23}	ω_s	$+314{,}159.27$
A_{31}	$-(n/2L\pi)\cdot[\cos((D_1+D_2)\pi) - \cos(D_2\pi)]$	$+5144.8566$
A_{32}	$-\omega_s$	$-314{,}159.27$
A_{33}	$-R/L$	$-3{,}134{,}796.24$

Similarly,

$$B(D) = [0\ \beta_2\ \beta_3\ 0\ 0\ 0\ ] \quad (4.15a)$$

$$\beta_2 = \frac{1}{2L} sin(d_1\pi) \tag{4.15b}$$

$$\beta_3 = -\frac{1}{L\pi} sin^2 \left(\frac{d_1\pi}{2}\right) \tag{4.15c}$$

Therefore, the averaged dynamics of the converter are completely described by state space form with duty-dependent coefficients. This is the GAM of the T-type Dual active bridge converter operating under Dual Phase Shifting modulation control strategy.

4.7.5 Small-Signal Modelling

By introducing small perturbations around the steady-state operating point:

$$d_1 = D_1 + d\hat{}_1 ; d_2 = D_2 + d\hat{}_2 \tag{4.16}$$

Applying linearised trigonometric expansions and neglecting second-order terms, the small-signal state-space model is obtained.

We have the small-signal

$$X = [\langle v\hat{}_o \rangle \langle \hat{i}_{L1R} \rangle \langle \hat{i}_{L1i} \rangle], U = [\langle d\hat{}_1 \rangle \langle d\hat{}_2 \rangle] \tag{4.17}$$

The state-space equation is

$$\dot{X} = AX + BU \tag{4.18}$$

$$A = \left[\begin{matrix} \frac{-1}{RC_0} & \frac{2n}{C_0\pi}\left(sin\, sin\left[(D_1+D_2)\pi\right] - sin(D_2\pi)\right) & \frac{2n}{C_0\pi}\left(cos\, cos\left[(D_1+D_2)\pi\right] - cos(D_2\pi)\right) & \frac{-n}{2L\pi}\left(\\ sin\, sin\left[(D_1+D_2)\pi\right] - sin(D_2\pi)\right) & \frac{-R}{L} & w_s & \frac{-n}{2L\pi}\left(cos\, cos\left[(D_1+D_2)\pi\right] \\ - cos(D_2\pi)\right) & -w_s & \frac{-R}{L} & \end{matrix}\right] \tag{4.19}$$

$$B = \left[\begin{matrix} \frac{2n}{C_0}\left(L_{1R}\, cos\, cos\left[(D_1+D_2)\pi\right] - I_{L1i} sin\pi(D_1+D_2)\right) & \frac{2n}{C_0}\left(sinD_2\pi - sin\, sin\, \pi(D_1+D_2)\right)I_{L1i} - (cos\pi D_2 \\ + cos\pi(D_1+D_2))I_{L1R} & \frac{1}{2L_1}\left[V_{in} cos(D_1\pi) - nV_o cos\pi(D_1+D_2)\right] & \frac{nV_o}{2L}\left(cos\, cos\left[(D_1\right.\right. \\ \left.\left.+D_2)\pi\right] + cos(D_2\pi)\right) & \frac{1}{2L_1}\left[nV_o sin\left[\pi(D_1+D_2)\right] - V_{in} sin(D_1\pi)\right] & \frac{nV_o}{2L}\left(sin\, sin\left[(D_1\right.\right. \\ \left.\left.+D_2)\pi\right] - sin(D_2\pi)\right) & & \end{matrix}\right] \tag{4.20}$$

where the output matrix is C = [1 0 0], D = 0, and the open-loop duty-to-output transfer

$$T(s) = \frac{L(s)}{1 + L(s)} = \frac{K_1(s)G_{vd1}(s) + K_2(s)G_{vd2}(s)}{1 + K_1(s)G_{vd1}(s) + K_2(s)G_{vd2}(s)} \tag{4.24}$$

function and I_L, I_R are steady-state harmonic current components, V_{IN} is input voltage, V_O is output voltage.

$$G_{vd}(s) = C(sI - A)^{-1}B + D \tag{4.21}$$

4.7.6 Closed-Loop System

The Proportional Integral controller regulates the output voltage by adjusting the duty ratios from both bridges based on feedback. The control law is:

$$T(s) = C(sI - A_{cl})^{-1}B_{cl} \tag{4.22}$$

$$L(s) = K_1(s)G_{vd1}(s) + K_2(s)G_{vd2}(s) \tag{4.23}$$

$$A_{cl} = \begin{matrix} -100.0000 & 0.0000 & -6564.8371 \\ -357{,}977.4262 & -3{,}134{,}796.2382 & +314{,}159.2654 \\ +159{,}632.7293 & -314{,}159.2654 & -3{,}134{,}796.2382 \end{matrix}]$$

$$B_{cl} = \begin{matrix} 0.0000 \\ [+357{,}977.4262] \\ -154{,}487.8726 \end{matrix}$$

$$T(s) = \frac{1.014\times10^{9}\, s^2 + 3.928\times10^{15}\, s + 3.918\times10^{19}}{s^4 + 6.270\times10^{6}\, s^3 + 9.927\times10^{12}\, s^2 + 5.026\times10^{15}\, s + 3.918\times10^{19}} \tag{4.25}$$

$$det(sI - A_{cl}) = det(sI - A)(1 + K^{T}C(sI - A)^{-1}B)$$

$$= s^3 + 6.2697\times10^{6}\, s^2 + 9.9263\times10^{12}\, s + 1.0984\times10^{15}$$

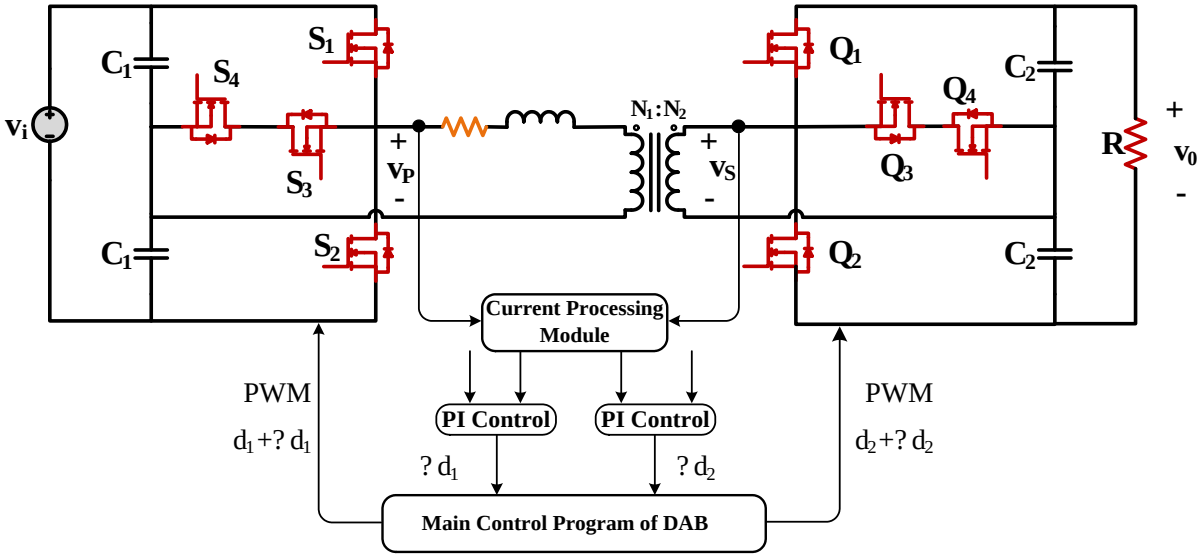

Fig. 4.7: Block Diagram of Closed-Loop T-Type Dual Active Bridge System with Proportional Integral Controllers

4.8 Simulation Parameters and Results

4.8.1 Open-Loop T-Type Dual Active Bridge Converter

Table 4.3: Open-Loop T-Type Dual Active Bridge Simulation Parameters

Parameter	Value
Input Voltage (Vi)	400 V
Output Voltage (Vo)	400 V
Power (P)	2 kW
Switching Frequency (fs)	50 kHz
Leakage Inductance (L)	35 µH
DC Link Capacitors (C_1, C_2)	300 µF

The open-loop simulation results are presented below.

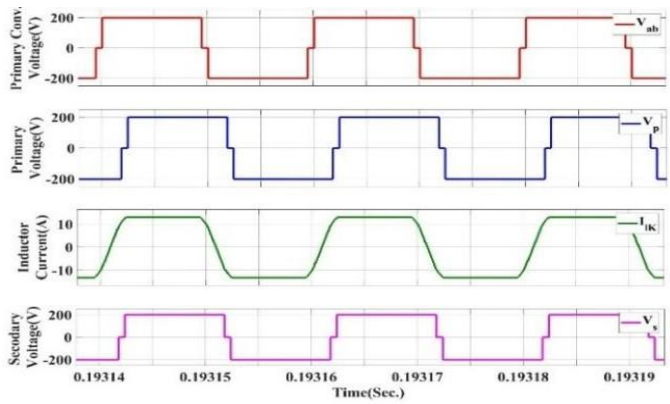

Fig. 4.8: Open-Loop T-Type Dual active bridge — (i) Primary Voltage; (ii) Transformer Primary Voltage Vp; (iii) Inductor Current; (iv) Secondary Voltage

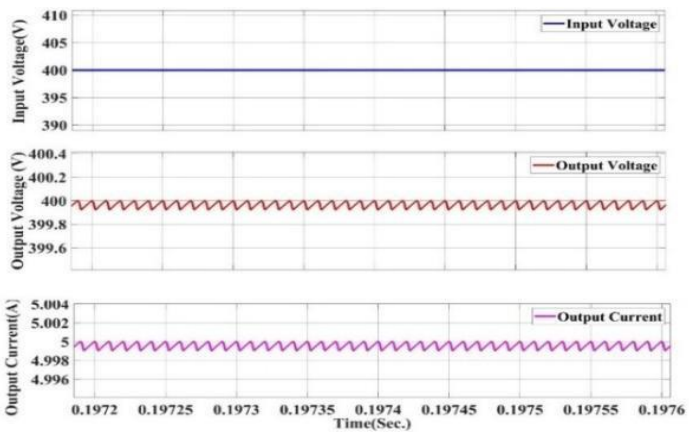

Fig. 4.9: Open-Loop T-Type Dual active bridge — (i) Input Voltage; (ii) Output Voltage; (iii) Output Current

During operation the input voltage waveform is steady. This means the converter is powered by a steady DC supply. The input current waveform, which is a function of the Dual active bridge converter switching action, indicates a smooth and controlled power transfer with limited current ripple.

4.8.2 Closed-Loop T-Type Dual Active Bridge Converter

Table 4.4: Closed-Loop T-Type Dual Active Bridge Simulation Parameters

Parameter	Value
Input Voltage (Vi)	1000 V
DC Link Capacitors (C_1, C_2)	100 µF
Inductance (L)	31.9 µH

Parameter	Value
Turns Ratio (N1:N2)	1:1.4
Load Resistance (R)	100 Ω

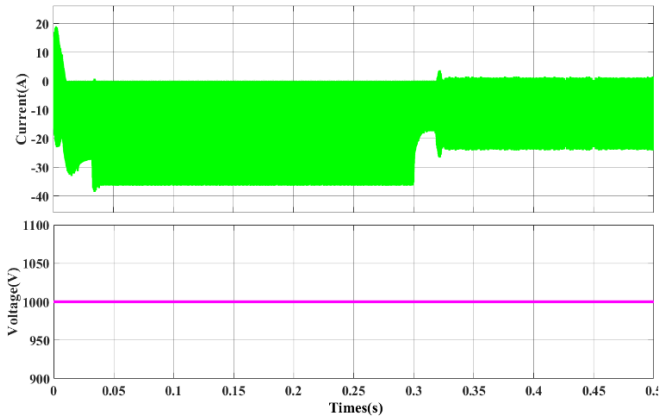

Fig. 4.10: Closed-Loop T-Type Dual active bridge — (i) Input Current; (ii) Input Voltage

During operation, the input voltage is kept at a desired level, which means the closed loop controller has good voltage regulation. Input current variation is smooth, which confirms stable and efficient power transfer with limited current ripple.

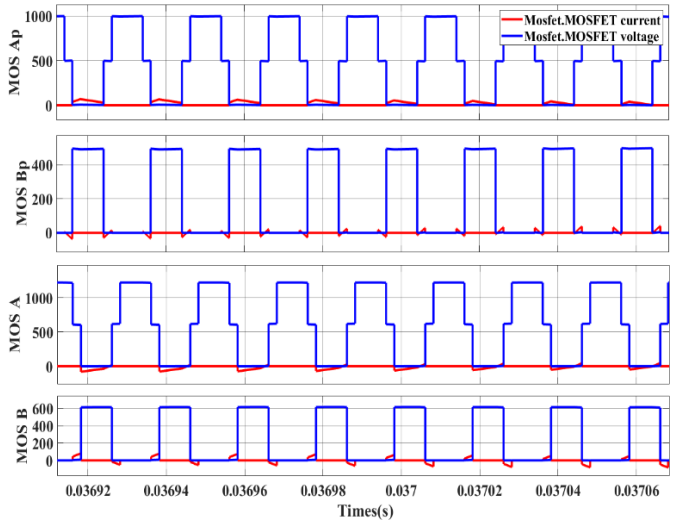

Fig. 4.11: Closed-Loop T-Type Dual active bridge — MOSFET Voltage Waveforms: (i) MOS Ap; (ii) MOS Bp; (iii) MOS A; (iv) MOS B

The voltage waveforms of the MOSFETs clearly show the switching action of the T-Type Dual active bridge converter in every operation cycle. The smooth current variation

verifies the ability of the proposed converter to operate stably with high power transfer capability and low switching stress.

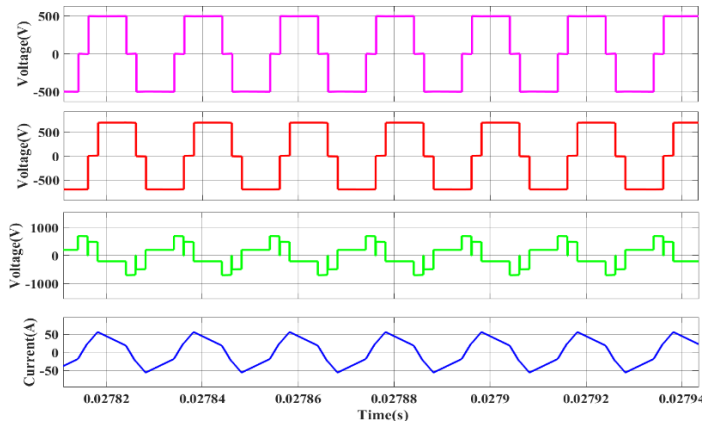

Fig. 4.12: Closed-Loop T-Type Dual active bridge — (i) Primary Voltage Vp; (ii) Transformer-Side Primary Voltage; (iii) Impedance Voltage Drop; (iv) Inductor Current

The above figure shows the 3-level voltage in the primary voltage, and similarly, along the impedance. The current shows the charging and discharging behaviour of the inductor current, which is also the primary current.

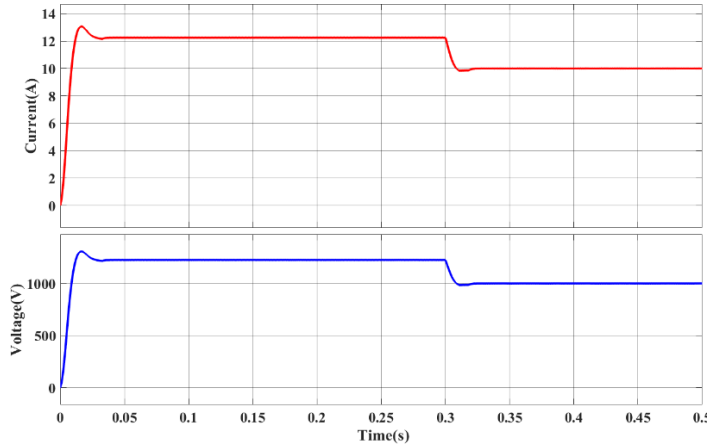

Figure 4.13: Closed-Loop T-Type Dual active bridge — (i) Output Current; (ii) Output Voltage

The start-up process shows that the output voltage and current rise smoothly and rapidly reach the desired values, indicating the stability of the T-Type Dual active bridge converter. During load change, small variation is observed and both waveforms stabilise confirming good dynamic response and effective voltage regulation.

4.9 Conclusion

This chapter studied a T-Type Dual Active Bridge (Dual active bridge) converter with dual phase-shift (Dual Phase Shifting) control for electric vehicle and DC-grid applications. The converter was analysed based on a Generalised State-Space Averaging (GSSA) technique, which helps to understand the switching converter behaviour with good accuracy and less computational complexity at different operating conditions.

The proposed multilevel Dual active bridge converter has the advantages of less current stress and circulating power as compared with the conventional Dual active bridge converter. Simulation results depicting stable working, faster response, and less overshoot, establishing the performance of the designed system for practical EV charging applications.

CHAPTER 5: CUK CONVERTER AND PFC

5.1 Introduction

The Ćuk converter is a versatile DC-DC converter topology featuring both the step-up (boost) and step-down (buck) converter topologies. It is named after Dr. Slobodan Ćuk who developed the topology in late 1970s. The Ćuk converter has the advantages of continuous input and output currents, lower EMI and can work in a wide range of input voltages. These features make it attractive for power conversion applications where effective energy management and low EMI are critical[2].

The operation principle relies on an inductor-capacitor (LC) network that preserves the energy transfer while switching between two states. In ON state, the input inductor stores energy and load is powered by output capacitor.In the OFF state, the input inductor releases its stored energy to the output capacitor, continuing to power the load. This energy transfer mechanism lowers overall ripple and EMI emission [3].

5.2 Overview of Power Factor Correction

Power Factor Correction (PFC) is a very important concept in the modern power electronics and systems and electrical systems. Power factor is the real power divided by apparent power [3],[5].:

$$Power\ factor = \frac{Real\ Power}{Apparent\ power} \tag{5.1}$$

A power factor close to unity indicates efficient utilisation of power. Power factor can be bad for two main reasons: displacement and distortion. Now there is displacement when the current and voltage are out of phase:

$$PF_{\{\{displacement\}\}} = cos(\theta_V - \theta_I) \tag{5.2}$$

Distortion occurs when the current waveform is non-sinusoidal. Total Harmonic Distortion (THD) and distortion power factor are:

$$THD = \frac{RMS\ Harmonic\ current}{RMS\ Fundamental\ current} \tag{5.3}$$

$$PF_{distortion} = \frac{1}{\sqrt{(1 + THD^2}} \tag{5.4}$$

The active PFC is a more advanced technique and is widely used in modern power electronic systems. It employs controlled semiconductor switches and converter circuits to shape the input current to follow the input voltage waveform, so as to achieve a power factor near to unity and reduce Total Harmonic Distortion (THD) [3],[5].

5.3 Conventional PFC Techniques

Passive PFC employs a low pass filter designed to remove higher order harmonics, leaving only the 50Hz fundamental frequency if all goes well. It is not very efficient in terms of power factor improvement and impractical for high power applications due to the loss of efficiency, size and weight of the passive components required [1],[2].

Table 5.1: Comparison of Active PFC and Passive PFC

Parameter	Active PFC	Passive PFC
Working Principle	Switching converters and semiconductor devices	Passive components (inductors, capacitors)
Power Factor	Very high (≈1)	Moderate improvement
Harmonics	Very low THD	Higher THD
Efficiency	High	Moderate
Size	Compact	Bulky
Complexity	Complex control circuit	Simple design
Cost	Higher	Lower
Applications	EV chargers, SMPS, data centers	Low-power applications

5.4 Advantages of Cuk Converter

The Cuk converter offers several advantages over conventional DC-DC topologies[1]-[6]:

- Continuous input current → Low input ripple and better power quality
- Continuous output current → Smooth output voltage and current
- Inherent buck–boost operation → Output can be higher or lower than input
- No inrush current problem → Input capacitor is not directly connected to the source
- Lower switching stress on MOSFET and diode
- Lower EMI and RFI due to smooth current waveform
- Smaller input EMI filter required
- Lower peak current compared to Boost and Buck-Boost
- Better suitability for PFC applications
- High power factor and low Total Harmonic Distortionachievable
- Better performance under wide input voltage variation
- Higher reliability and longer component life
- Good efficiency over a wide load range
- Stable operation in both CCM and DCM

5.5 Working of Cuk Converter

5.5.1 Mode 1: Switch ON, Diode OFF

When the switch is closed (S=1, D=0), applying KVL and KCL to the circuit:

1. Applying KVL:

$$-v_{in} + v_{L1} = 0$$

$$L_1 \frac{di_{L1}}{dt} = v_{in}$$

$$\frac{di_{L_1}}{dt} = \frac{v_{in}}{L_1} \tag{5.5}$$

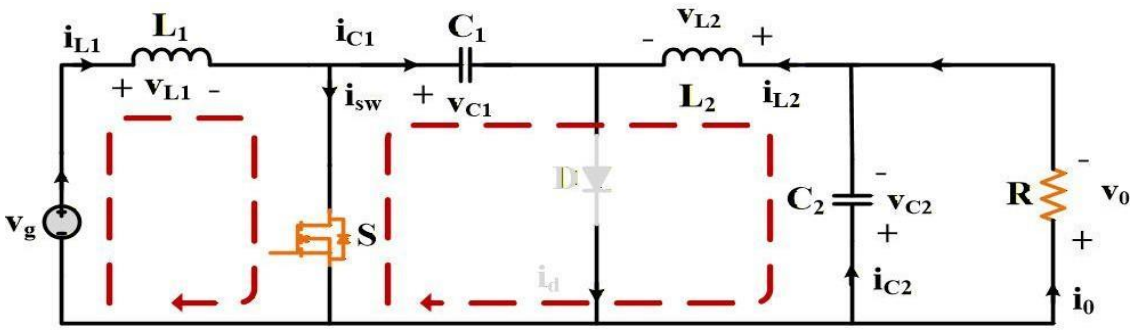

Fig. 5.1: Cuk Converter Mode 1 Circuit Diagram (Switch ON)

2. Applying KVL:

$$v_{C_2} + v_{L2} + v_{C_1} = 0$$
$$v_{L_2} = v_{C1} - v_{C_2}$$
$$L_2 \frac{diL2}{dt} = v_{C1} - v_{C_2}$$
$$\frac{di_{L_2}}{dt} = \frac{v_{C1}}{L_2} - \frac{v_{C_2}}{L_2} \tag{5.6}$$

3. Applying KCL:

$$i_{C1} + i_{L_2} = 0$$
$$i_{C_1} = -i_{L_2}$$
$$C_1 \frac{dV_{C1}}{dt} = -i_{L_2}$$
$$\frac{dV_{C_1}}{dt} = -\frac{i_{L_2}}{C_1} \tag{5.7}$$

4. Applying KCL:

$$i_{C2} + i_0 = i_{L_2}$$
$$i_{C2} = i_{L_2} - i_0$$
$$C_2 \frac{dV_{C2}}{dt} = i_{L_2} - i_0$$
$$\frac{dV_{C2}}{dt} = \frac{i_{L2}}{C_2} - \frac{i_0}{C_2}$$
$$\frac{dV_{C2}}{dt} = \frac{i_{L2}}{C_2} - \frac{v_0}{RC_2}$$
$$\frac{dV_{C2}}{dt} = \frac{i_{L2}}{C_2} - \frac{v_{C2}}{RC_2} \tag{5.8}$$

5.5.2 Mode 2: Switch OFF, Diode ON

When the switch is open (S=0, D=1), applying KVL and KCL to the circuit:

5. Applying KVL:

$$-v_{in} + v_{L_1} + v_{C_1} = 0$$
$$v_{L_1} = v_{in} - v_{C_1}$$
$$L_1 \frac{di_{L1}}{dt} = v_{in} - v_{C_1}$$
$$\frac{di_{L_1}}{dt} = -\frac{v_{C1}}{L_1} + \frac{v_{in}}{L_1} \tag{5.9}$$

6. Applying KVL:

$$v_{L_2} + v_{C_2} = 0$$
$$L_2 \frac{di_{L_2}}{dt} = -v_{C_2}$$
$$\frac{di_{L2}}{dt} = -\frac{v_{C2}}{L_2} \tag{5.10}$$

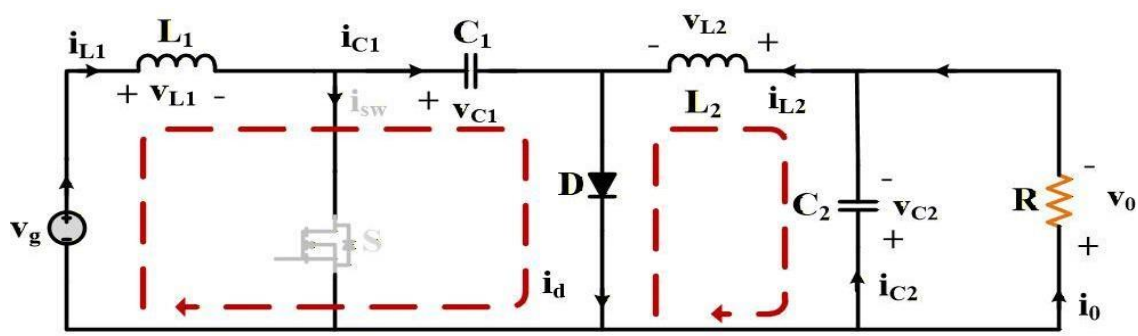

Fig. 5.2: Cuk Converter Mode 2 Circuit Diagram (Switch OFF)

7. Applying KCL:

$$i_{C_1} = i_{L_1}$$
$$C_1 \frac{dvC1}{dt} = i_{L_1}$$
$$\frac{dv_{C_1}}{dt} = \frac{i_{L_1}}{C_1} \tag{5.11}$$

8. Applying KCL:

$$i_{C_2} + i_0 = i_{L_2}$$
$$i_{C_2} = i_{L_2} - i_0$$
$$C_2 \frac{dv_{C_2}}{dt} = i_{L_2} - \frac{v_{C2}}{R}$$
$$\frac{dv_{C_2}}{dt} = \frac{i_{L_2}}{C_2} - \frac{v_{C2}}{RC_2} \tag{5.12}$$

5.6 State-Space Average Model of Cuk Converter

Combining both modes using state-space averaging:

$$\frac{d\underline{i}_{L_1}}{dt} = \frac{V_{in}}{L_1} - \frac{(1-\underline{d})\underline{v}_{C_1}}{L_1} \tag{5.13}$$

$$\frac{d\underline{i}_{L_2}}{dt} = \frac{(\underline{d})\underline{v}_{C_1}}{L_2} - \frac{\underline{v}_{C_2}}{L_2} \tag{5.14}$$

$$\frac{d\underline{v}_{C_1}}{dt} = -\frac{(\underline{d})\underline{i}_{L_2}}{C_1} + \frac{(1-\underline{d})\underline{i}_{L_1}}{C_1} \tag{5.15}$$

$$\frac{d\underline{v}_{C_2}}{dt} = \frac{\underline{i}_{L_2}}{C_2} - \frac{(\underline{v}_{C_2})}{RC_2} \tag{5.16}$$

5.6.1 Perturbation and Linearisation

After applying small-signal perturbation and neglecting higher-order terms, the linearised small-signal model is:

$$\frac{d\hat{\underline{\iota}}_{L1}}{dt} = -\frac{(1-D)\hat{v}_{C1}}{L_1} + \frac{V_{C_1}}{L_1}\hat{d} \tag{5.17}$$

$$\frac{d\hat{\underline{\iota}}_{L2}}{dt} = \frac{V_{C1}}{L_2} * \hat{d} + \frac{\hat{v}_{C1}}{L_2} * D - \frac{1}{L_2} * \hat{v}_{C2} \tag{5.18}$$

$$\frac{d\hat{v}_{C1}}{dt} = -\frac{\hat{d} * I_{L2}}{C_1} - \frac{D * \hat{\iota}_{L2}}{C_1} + \frac{(1-D)\hat{\iota}_{L1}}{C_1} - \frac{\hat{d} * I_{L1}}{C_1} \tag{5.19}$$

$$\frac{d\hat{v}_{C2}}{dt} = \frac{\hat{\iota}_{L2}}{C_2} - \frac{\hat{v}_{C2}}{R * C_2} \tag{5.20}$$

The DC voltage conversion ratio of the Cuk converter is:

$$V_o = -\frac{D}{1-D}V_{in} \tag{5.21}$$

5.7 Design of Open-Loop Cuk Converter

The open-loop Cuk converter is designed for a 220 V RMS AC input at 30 kHz switching frequency. The component values are calculated as follows:

$$L_1 = \frac{DV_s}{\Delta i_{l1} * f_{sw}} = .271\text{mH}$$

$$L_2 = \frac{DV_s}{\Delta i_{l2} * f_{sw}} = 2.0\text{mH}$$

$$C_1 = \frac{D\,|V_O|}{\Delta V_{c1} R f_{sw}} = 1.75\mu H$$

$$C_2 = \frac{1-D}{8\,L_2 \frac{\Delta V_O}{V_O} f_{sw}^2} = 111.11\ \mu H \qquad (5.25)$$

Table 5.2: Open-Loop Cuk Converter Parameters

S.No.	Parameter	Value
1	AC Voltage Source (RMS)	220 V
2	Input Voltage to Converter	197.8 V
3	Duty Cycle (D)	0.63
4	Inductor Current iL1	9.8 A
5	Inductance L1	0.271 mH
6	Capacitance C1	1.75 µF
7	Inductance L2	2.0 mH
8	Inductor Current iL2	4.51 A
9	Capacitance C2	111.11 µF
10	Output Voltage Vo	341 V
11	Switching Frequency fsw	30 kHz

Open-loop simulation results:

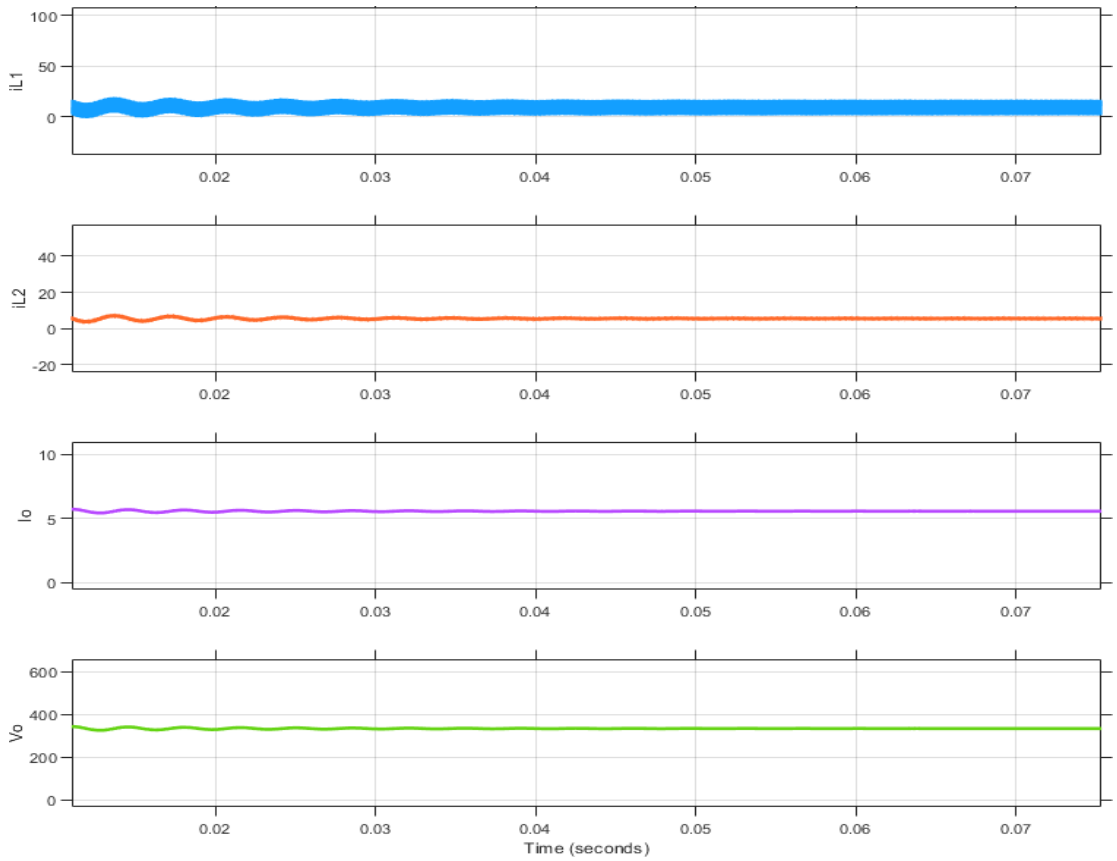

Figure 5.3: Open-Loop Cuk Converter — Inductor Current iL1 vs. Time

Figure 5.4: Open-Loop Cuk Converter — Inductor Current iL2 vs. Time

Figure 5.5: Open-Loop Cuk Converter — Output Current Io vs. Time

Figure 5.6: Open-Loop Cuk Converter — Output Voltage Vo vs. Time

5.8 Closed-Loop Cuk-PFC

A **closed-loop system** is a control system in which the output is continuously measured and fed back to the controller, and the controller automatically corrects the input to keep the output at the desired value.

Output is checked → Error is calculated → System corrects itself automatically.
Closed-Loop in Cuk PFC (EV Charger)

- You set DC link voltage = 350V
- Actual voltage is measured
- Error = (350V – Measured V)
- Proportional Integral Controller adjusts duty cycle
- Cuk converter output corrects itself

This keeps DC link constant even if AC input changes.
In power converters:

$$e(t) = V_{ref} - V_{out} \tag{5.26}$$

The controller adjusts:

- **Duty cycle (D)** in PWM converters
- **Switching frequency (f_s)** in resonant converters

This ensures:

$$V_{out} = V_{ref}\ despite\ load\ and\ input\ variations$$

A closed-loop control system is essential in power electronic converters because it provides accurate output regulation, effective disturbance rejection, system stability, fast dynamic response, and protection against over-voltage and over-current conditions. By continuously adjusting the duty cycle or switching frequency based on output feedback, it ensures constant voltage/current under line, load, and parameter variations. In PFC applications, closed loop is mandatory to enforce sinusoidal input current and maintain high power factor with low harmonic distortion [4].

The controlled output voltage (V_o) generation depends on the error voltage (V_e) and proportional integral (Proportional Integral) controller as,

$$V_O(k) = V_O(k-1) + k_{p1}\{V_e(k) - V_e(k-1)\} + k_{l1}V_e(k) \tag{5.27}$$

Where k_{p1} and k_{i1} are proportional and integral gain respectively.

The reference input current is generated as the product of the voltage loop output and the normalised sinusoidal template:

$$i_{ref} = V_c \times |\, v_{in} \,| \tag{5.28}$$

PWM pulse generation: If the modulating signal is less than Vo(t), the switch is ON; otherwise, the switch is OFF.

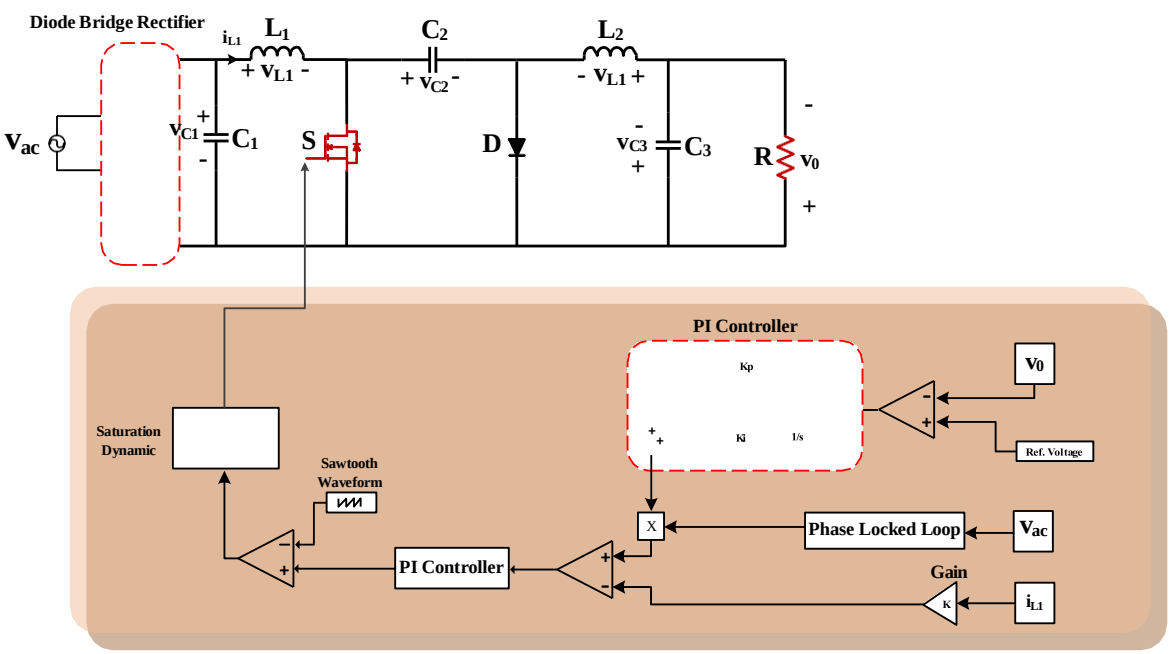

Fig. 5.7: Configuration of Cuk-PFC Converter with Dual-Loop Control

5.9 Cuk-PFC Component Design

The Cuk-PFC converter is designed for 220 V RMS AC input, 350 V regulated DC link output, and 30 kHz switching frequency with 20% allowable inductor ripple current:

(f_{sw}=30KHz)

$\Delta I_{l1,2} = 20\%$ of inductor current

$$L_1 = \frac{V_S * V_S * D}{P_i * (0.2) * f_{sw}}$$

= 2.54 *1.25

= 3.17mH

$$L_2 = \frac{V_S * V_S * V_O * D}{P_i * (2 * V_S * f_{sw})}$$

=.561mh *1.25

=7.01mH

$$C_1 = \frac{V_O}{K * (\sqrt{2} * V_S) * (\sqrt{2} V_S + V_O)}$$ (Tank Capacitor)

= .56 µH

This capacitor is the main capacitor in the Cuk converter for energy transfer.

K is the ripple voltage percentage taken as 10% [3].

$$C_d = \frac{P_i}{2w_l \alpha V_o * V_0}$$

$$= 900\mu H \tag{5.31}$$

Table 5.3: Closed-Loop Cuk-PFC Parameters

S.No.	Parameter	Value
1	AC Voltage Source (RMS)	220 V
2	AC Input Current (Iac)	52.94 A
3	Input Voltage to Converter	197.8 V
4	Duty Cycle (D)	Varies (controlled)
5	Inductor Current iL1	14.8 A
6	Inductance L1	3.17 mH
7	Capacitance C1	0.56 µF
8	Inductance L2	7.01 mH
9	Inductor Current iL2	9.5 A
10	Capacitance C2 (Cd)	910 µF
11	Output Voltage Vo	351 V
12	Switching Frequency fsw	30 kHz

Closed-loop simulation results:

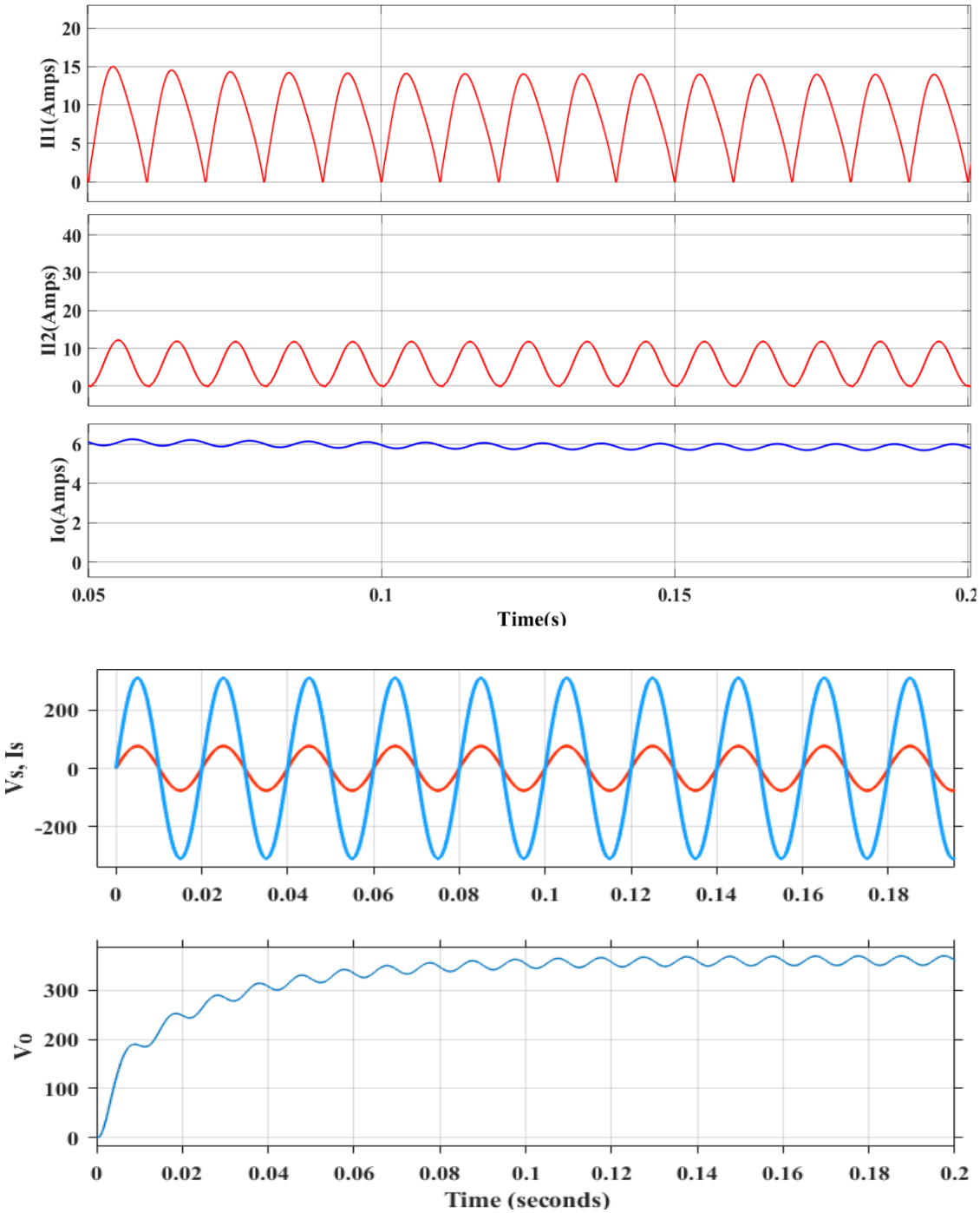

Fig. 5.8: Closed-Loop Cuk-PFC Simulation Results — (a) Inductor Current I_{l1}; (b) Inductor Current I_{l2}; (c) Source Voltage Vs and Source Current Is in Phase (Unity PF); (d) Output Voltage Vo.

5.10 Conclusion

The Ćuk converter is a versatile DC-DC topology that is suitable for precision power and power-factor-correction (PFC) applications. Its inherent buck-boost operation, low ripple, low EMI and continuous input and output currents make it suitable for EV charging applications. The duty cycle is fixed and cannot compensate for changes in load, input voltage, or component tolerances, resulting in poor voltage regulation.

The closed-loop Ćuk converter continuously senses the output voltage and/or inductor current, compares it with a reference, and adjusts the duty cycle accordingly. The dual-loop (voltage + current) control system maintains a stable 350 V DC link, sinusoidal input current, and achieves Total Harmonic Distortion= 11%, demonstrating excellent dynamic response against line and load disturbances.

CHAPTER 6: CONCLUSION AND FUTURE SCOPE

The This thesis set out to evaluate the performance of two advanced power electronic converter topologies — the T-Type Dual Active Bridge converter and the Cuk-PFC converter — for electric vehicle charging applications. The analysis has demonstrated that both converters offer meaningful performance advantages over the conventional topologies they are intended to replace.

The T-Type Dual active bridge, operating under Dual Phase Shifting modulation with Proportional Integral voltage control, achieves stable and efficient power transfer with reduced switching losses and improved waveform quality compared to the conventional two-level Dual active bridge. The Generalised Averaging Model developed in this work provides an accurate and computationally efficient representation of the converter's dynamics, suitable for control design and performance prediction.

The Cuk-PFC converter, with its inherently continuous input and output currents, achieves excellent power factor correction and low harmonic distortion, meeting the power quality requirements of modern EV charging standards. Its performance compares favourably with the boost PFC topology that dominates current designs, particularly in applications where electromagnetic interference is a concern.

Several directions for future work suggest themselves. Hardware implementation and experimental validation of both converters would confirm the simulation results and reveal any discrepancies attributable to non-ideal component behaviour. Optimisation of the Dual Phase Shifting modulation parameters across the full operating range — including varying input voltage and load — using model predictive control or machine learning techniques could further improve efficiency. Extension of the T-Type Dual active bridge analysis to three-phase topologies would address higher power levels. And integration of both converters into a complete two-stage EV charger system, with coordinated control across both stages, would demonstrate their combined performance in a realistic application context.

REFERENCES

[1] S. K. Sahoo, A. K. Sinha and N. K. Kishore, “Control Techniques in AC, DC, and Hybrid AC–DC Microgrid: A Review,” IEEE Trans. Emerg. Sel. Topics Power Electron., vol. 6, no. 2, pp. 738-759, 2018.

[2] D. Das, S. Mishra and B. Singh, “Design Architecture for Continuous Time Control of Dual Active Bridge Converter,” IEEE Trans. Emerg. Sel. Topics Power Electron, 2020.

[3] C. P. Kumar, P. Alam and A. Jamatia, “Modelling and Control of Dual-Active-Bridge Converter for GridConnected PV System,” in International Conference on Power Electronics & IoT Applications in Renewable Energy and its Control (PARC), Mathura, Uttar Pradesh, India, 2020, pp. 461-466

[4] Biao Zhao, Qiang Song, Wenhua Liu, and Yandong Sun, “Overview of Dual-Active-Bridge Isolated Bidirectional DC-DC Converter for High Frequency-Link Power-Conversion System,” IEEE Trans. Power Electron., vol. 29, no. 8, pp.4091-4106, Aug. 2014.

[5] M. H. Kheraluwala, R. W. Gascoigne, D. M. Divan, and E. D. Baumann, “Performance characterization of a high-power dual active bridge dc to dc converter,” IEEE Trans. Ind. Appl., vol. 28, no. 6, pp. 1294- 1301, Nov./Dec. 1992.

[6] M. Fiaz and J. Kimball, “Generalized average modelling techniques for dual active bridge converters,” IEEE Access, vol. 10, pp. 56 789–56 799, 2022.

[7] A. Pal, S. Kapat, K. Jha, and A. Tiwari, “Discrete-time framework for digital control design in a high-frequency dual active bridge converter,” Proceedings of the International Conference on Power Electronics, pp. 1–6, 2018

[8] Y. Li, Y. Wang, Y. Guan, and D. Xu, “Design and analysis of integrated bidirectional dc-dc converter for energy storage systems,” IEEE Transactions on Industrial Electronics, vol. 71, no. 9, pp. 10 568–10 579, 2024.

[9]] Y. Chen and X. Wang, “Generalized average modelling of t-type dab converters for grid-connected applications,” IEEE Transactions on Industrial Electronics, vol. 70, no. 4, pp. 5678–5689, 2023

[10]] Y. Liu, X. Wang, W. Qian, and F. Z. Peng, “A simple phase-shift modulation using parabolic carrier for dual active bridge dc-dc converter,” IEEE Transactions on Power Electronics, vol. 35, no. 1, pp. 123–134, 2020.

[11] S. Rolak and J. Biela, “Triple-phase-shift modulation techniques for t-type dual active bridge converters,” IEEE Transactions on Power Electronics, vol. 37, no. 12, pp. 13 456–13 467, 2022.

[12] A. K. Gupta, D. Singh, P. Kant and S. K. Dube, "Steady-State and Small-Signal Analysis of a T-Type Dual Active Bridge Converter Using a Generalised Averaging Approach," 2025 12th National Power Electronics Conference (NPEC), Kozhikode, India, 2025.

[13] Hart, Daniel W. 2011. Power Electronics International ed. New York: McGraw-Hill.

[14] R. W. Erickson and D. Maksimovic, Fundamentals of Power Electronics, 2nd ed. Kluwer Academic Publishers, 2001.

[15] R. Pandey and B. Singh, “A Power Factor Corrected LLC Resonant Converter for Electric Vehicle Charger Using Cuk Converter,” Proceedings of IEEE Conference, pp. 1–6, 2018.

[16] S. Cuk and R. D. Middlebrook, "A general unified approach to modelling switching DC-to-DC converters in discontinuous conduction mode," IEEE Transactions on Power Electronics, vol. 2, no. 2, pp. 96-106, 1987.

[17] A. Jha and B. Singh, “Cuk PFC Converter for High Brightness LED Driver with Brightness Control,” IEEE Conference Proceedings, pp. 1–6, 2016.

[18] S. S. Williamson, A. K. Rathore and F. Musavi, “Industrial electronics for electric transportation: Current state-of-the-art and future challenges,” IEEE Transactions on Industrial Electronics, vol. 62, no. 5, pp. 3021-32, 20